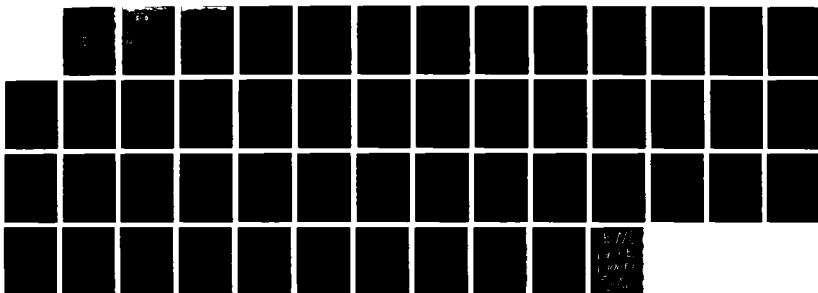AD-A191 857   MOLECULAR SOURCES OF IONOSPHERIC HOLES(U) SMITHSONIAN   1/1
              ASTROPHYSICAL OBSERVATORY CAMBRIDGE MA S L GUBERMAN
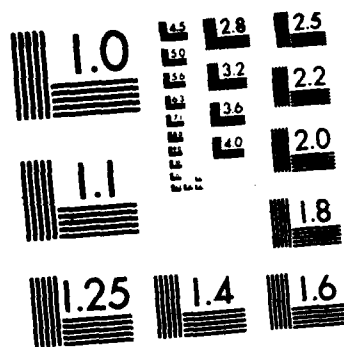   19 NOV 87 AFOSR-TR-88-0064 AFOSR-84-0109

UNCLASSIFIED   F/G 20/5   NL

MICROCOPY RESOLUTION TEST CHART

NATIONAL BUREAU OF STANDARDS-1963-A

AD-A191 857

REPORT DOCUMENTATION PAGE

1b. RESTRICTIVE MARKINGS	
2a. SECURITY CLASSIFICATION AUTHORITY	3. DISTRIBUTION/AVAILABILITY OF REPORT
2b. DECLASSIFICATION/DOWNGRADING SCHEDULE	Approved for public release; distribution unlimited
4. PERFORMING ORGANIZATION REPORT NUMBER(S)	5. MONITORING ORGANIZATION REPORT NUMBER(S)
	AFOSR-TR- 88-0064

6a. NAME OF PERFORMING ORGANIZATION	6b. OFFICE SYMBOL (If applicable)	7a. NAME OF MONITORING ORGANIZATION
Smithsonian Astrophysical Observatory		AFOSR/NC
6c. ADDRESS (City, State and ZIP Code)		7b. ADDRESS (City, State and ZIP Code)
60 Garden Street Cambridge, MA 02138		Bldg. 410 Bolling AFB, DC 20332-6448

8a. NAME OF FUNDING/SPONSORING ORGANIZATION	8b. OFFICE SYMBOL (If applicable)	9. PROCUREMENT INSTRUMENT IDENTIFICATION NUMBER
AFOSR	NC	AFOSR-84-0109

8c. ADDRESS (City, State and ZIP Code)	10. SOURCE OF FUNDING NOS.			
Bldg. 410 Bolling AFB, DC 20332-6448	PROGRAM ELEMENT NO.	PROJECT NO.	TASK NO.	WORK UNIT NO.
	61102F	2303	B1	

11. TITLE (Include Security Classification)
MOLECULAR SOURCES OF IONOSPHERIC HOLES

12. PERSONAL AUTHOR(S)
Steven L. Guberman

13a. TYPE OF REPORT	13b. TIME COVERED	14. DATE OF REPORT (Yr., Mo., Day)	15. PAGE COUNT
FINAL REPORT	FROM 4/1/84 TO 9/30/87	1987 November 19	46

16. SUPPLEMENTARY NOTATION

17. COSATI CODES			18. SUBJECT TERMS (Continue on reverse if necessary and identify by block number)
FIELD	GROUP	SUB. GR.	Dissociatve recombination; electronic width; cross section; rate; autoionization

19. ABSTRACT (Continue on reverse if necessary and identify by block number)

The dissociative recombination of molecular ions with electrons determines many of the properties of the Earth's ionosphere under both quiescent and disturbed conditions. However, in spite of its importance, there has never been an experimental measurement of dissociatve recombination rates from individual excited ion vibrational levels. We have completed large scale ab initio calculations of cross sections and rates for the dissociative recombination of the molecular oxygen ion leading to excited oxygen atoms in the ^1S and ^1D states, the upper states of the well known green and red lines, respectively. Large scale wave functions having in excess of 100,000 terms have been calculated for the dissociative routes and accurate potential curves have

(over)

20. DISTRIBUTION/AVAILABILITY OF ABSTRACT	21. ABSTRACT SECURITY CLASSIFICATION
UNCLASSIFIED/UNLIMITED ☒ SAME AS RPT. ☒ DTIC USERS ☐	UNCLASSIFIED

22a. NAME OF RESPONSIBLE INDIVIDUAL	22b. TELEPHONE NUMBER (Include Area Code)	22c. OFFICE SYMBOL
Major Larry P. Davis	202/767-4960	NC

DD FORM 1473, 83 APR EDITION OF 1 JAN 73 IS OBSOLETE.

19.   been determined. A new method for calculating electronic autoionization widths using high Rydberg state wave functions to represent the inner part of the free electron wave function has been used and tested on the NO molecule where we have found that the widths can be calculated to an expected accuracy of about 15%. The widths have been used to determine dissociative recombination cross sections as a function of electron energy. Large windows have been discovered in the cross sections from excited vibrational levels. The windows, at which the cross sections drop precipitously, are due to the overlap of the peak in the continuum vibrational wave functions. the number of windows in the cross section from a particular ion vibrational level is given by the number of ion vibrational wave function nodes lying to the small internuclear distance side of the intersection point of the repulsive curve with the vibrational level undergoing recombination. A single dissociative route has been identified as the main channel leading to excited ^1S atoms while three routes have been shown to be important for the production of ^1D atoms. The production of ^1S atoms is very sensitive to vibrational excitation. The rate from the third vibrational level is about 80 times larger than the rate from the lowest vibrational level. For ^1D atoms the rate from $v=0$ is the largest and is about a factor of two larger than the rate from $v=2$.

C4

MOLECULAR SOURCES OF
IONOSPHERIC HOLES

AFOSR-84-0109

AFOSR-TR- 88-0064

Final Report

For the period 1 April 1984 through 30 September 1987

Principal Investigator
Dr. Steven L. Guberman

November 1987

Prepared for
Air Force Office of Scientific Research
Bolling AFB, D. C. 20332

Smithsonian Institution
Astrophysical Observatory
Cambridge, Massachusetts 02138

The Smithsonian Astrophysical Observatory
is a member of the
Harvard-Smithsonian Center for Astrophysics

88 2 24 138

TABLE OF CONTENTS

FINAL TECHNICAL REPORT

AFOSR-84-0109

MOLECULAR SOURCES OF IONOSPHERIC HOLES

For the period April 1, 1984 - September 31, 1987

I. Introduction

The dissociative recombination (DR) of molecular ions with electrons is an
important process determining the radiative characteristics and overall
energy balance of both the quiescent and perturbed ionosphere. The large
scale ionospheric electron depletion or hole that results after the launch
of large rockets has been attributed to DR.[1] The modelling of the detailed
role played by DR in the Earth's atmosphere has been hampered by the lack of
reliable rate constants. During the past 3 1/2 years we have performed large
scale ab initio calculations of the rate constants for the DR of O_2^+ with an
electron:

$$O_2^+ + e^- \rightarrow O + O. \tag{1}$$

The research has combined state of the art techniques in both bound state
calculations and scattering theory. The results provide a detailed
description of the variation of the DR rate constants for producing excited
states of O with ion vibrational excitation and electron temperature. In
addition to being an application to O_2^+ DR the research has involved the

1

development of new techniques for the accurate calculation of molecular electronic autoionization widths and potential energy curves. Results obtained from these new techniques are summarized in Sections II and III below. Section IV presents the cross section calculations and a discussion of the large windows which have been discovered in DR cross sections from excited ion vibrational levels. Results for the generation of both $O(^1S)$ and $O(^1D)$ atoms from DR are presented and compared to satellite observations in Section IV and the Appendix.

II. Wave Functions and Potential Curves

Potential curves determined previously[2,3] have been improved by using considerably larger basis sets and configuration interaction (CI) wave functions having a factor of 100 more terms than in the earlier studies. Briefly, the CI wave function is composed of configurations, each of which describes a possible distribution of the electrons in the molecular orbitals for that electronic state. For example, for the ground state of O_2, the most important configuration near the equilibrium internuclear separation is:

$$(1\sigma_g)^2(1\sigma_u)^2(2\sigma_g)^2(2\sigma_u)^2(3\sigma_g)^2(1\pi_u)^4(1\pi_g)^2 \qquad (2)$$

The 1σ and 2σ orbitals are mostly O atom 1s and 2s orbitals, respectively. The $3\sigma_g$ orbital is a bonding combination consisting mostly of the O atom 2p orbitals lying along the bonding axis. The $1\pi_u$ and $1\pi_g$ orbitals are out of plane bonding and antibonding orbitals respectively, consisting mostly of the O 2p orbitals that are perpendicular to the bonding axis. In the techniques used here, the orbitals in (2) are optimized for the electronic state of interest (in this example the ground state of O_2) in a large

2

calculation which includes all the configurations of the proper total symmetry) which can be formed by distributing the electrons in all the valence orbitals. The latter set would include the $3\sigma_u$ orbital which is not included in (2). In general, the 1σ orbitals, which do not participate in the bonding are constrained to remain doubly occupied. For the ground state of O_2 this procedure generates 14 terms or configurations. Each of the orbitals, ϕ_j, including those shown in (2), are expanded in a large set of Gaussian basis functions, χ_i,

$$\phi_j = \sum_i c_{j,i} \chi_i \qquad (3)$$

Both the coefficient in front of each configuration and the $c_{j,i}$ are optimized in multiconfiguration self consistent field (MCSCF) or in Complete Active Space Self Consistent Field (CASSCF) calculations.[4] In general, many of the χ_i in (3) consist of contractions of individual or primitive Gaussians[5] whose weighting coefficients have been determined in atomic calculations.[6] Since the orbitals are expanded in large basis sets, χ_i, the number of orbitals used in the MCSCF or CASSCF is only a subset of the full number of orbitals that can be formed from the basis set. The remaining orbitals are called virtual orbitals and are employed in the CI calculations to obtain even more accurate results than those from the MCSCF or CASSCF procedures. The CI wave functions are constructed by exciting electrons out of a small set of reference configurations into the virtual orbitals. The reference configurations usually consist of all the configurations needed to properly dissociate that particular state to the proper separated atoms limit. Taking at most one or two electrons from a reference configuration and promoting them to the virtual orbitals leads to a singles and doubles CI denoted CISD. The calculation of these large wave functions often having

3

more than 100,000 terms has been made possible in recent years by the development of direct CI techniques for solving for the mixing coefficients in front of each configuration.[7] The calculations used here employ these large scale wave functions and direct CI techniques. Calculations on several states of O_2 and N_2 provide examples of the sort of accuracy which can be expected with these techniques. Calculations on the ground state of O_2 using a basis set consisting of 6s,3p,2d and 1f type contracted Gaussians leads to a 228,036 term wave function. The calculated (experimental[8]) results are 1565.47(1580.19) for ω_e, 10.93(11.98cm^{-1}) for $\omega_e x_e$, and 2.2999(2.2819a_0) for R_e. For O_2, a series of vertical excitation energies have been calculated. The calculated (experimentally derived) results are 5.8982(5.90eV) for $^1\Sigma_u^-$, 6.1318(6.11eV) for $^3\Delta_u$, 6.2766(6.19eV) for $^3\Sigma_u^+$, and 8.66(8.61$\pm$0.05eV[9]) for $^3\Sigma_u^-$. All the experimental energies are derived[10] from Ref.8 except for $^3\Sigma_u^-$. These calculated vertical excitation energies deviate by no more than 0.09eV from experiment and indicate that the placement of the calculated repulsive curves relative to the ion should be highly accurate. For the ground state of N_2, 14 reference configurations (needed to properly dissociate the ground state to ^4S atoms) are used in the CI with a basis set of the same size leading to a CI wave function having 176,536 terms. The calculated (experimental[11]) spectroscopic constants are 2340.57(2356.56cm^{-1}) for ω_e, 14.27(14.3244cm^{-1}) for $\omega_e x_e$, and 2.0856(2.074347a_0) for the equilibrium internuclear distance, R_e.

The techniques described here have been applied to the important DR routes for the low ion vibrational levels. The results[12] indicate that a state of $^1\Sigma_u^+$ symmetry which crosses the ion between the large R turning points of v=1 and v=2 is the only state which leads to $O(^1S)$ atoms from the lowest 10 vibrational levels. On the other hand, potential curve considerations alone indicate that there are five states that can contribute

to $O(^1D)$ formation from the lowest ion vibrational levels: $1\,^1\Pi_g$, $1\,^3\Pi_g$, $1\,^3\Sigma_u^-$, $1\,^1\Sigma_u^+$, and $1\,^1\Delta_u$.[13] The results are described in more detail in the Appendix and Section IV.

III. Electronic Widths

The calculation of DR cross sections requires the calculation of the autoionization lifetimes or widths of the molecular states which cross into the electron-ion continuum. Techniques for calculating the widths have been developed with AFOSR support. The calculation of molecular electronic capture widths has historically been a difficult problem for quantum chemists. The width, Γ, is a matrix element of the Hamiltonian operator, H, given by Fermi's golden rule:

$$\Gamma(R) = 2\pi\rho\,|\langle\Psi_f|H|\Psi_I^c\rangle|^2 \tag{4}$$

where Ψ_I^c is the wave function of the properly antisymmetrized product of a "free" electron in a coulomb like orbital and the wave function for the ion. Ψ_f is the electronic wave function for the neutral state which describes the products of reaction (1) or the entrance channel of reaction (4), R is the internuclear distance, and ρ is the density of states. In order to do the integral in (4) both the coulomb orbitals and the bound orbitals must be expanded about a common origin. With the coulomb orbital placed at the molecular midpoint, the bound orbitals, which have most of their amplitude near the nuclei, must instead be represented at the molecular midpoint by a very large slowly convergent basis function expansion. Similar difficulties arise in solving for the optimum coulomb orbital in the field of the bound

electrons. Under AFOSR support, these problems have been overcome by using Rydberg orbitals with high principal quantum numbers, n, to describe the coulomb orbital. Except for the coulomb orbital, all the orbitals in (4) are bound and have large amplitude only near the molecule. As a result, it is only important to know the amplitude of the coulomb orbital near the molecule. The inner part of coulomb orbitals are well known to be very similar to the inner part of high Rydberg orbitals.[14] With the coulomb orbital represented as a high Rydberg orbital all the orbitals in (4) are then bound and are represented in terms of Gaussian basis functions. Large slowly converging expansions are not needed. Since Gaussians have the property that the product of two Gaussians on different centers is just a third Gaussian located along the line connecting the first two, the matrix element in (4) can be easily evaluated.

The Rydberg orbitals for the Π states of NO have been represented by a set of 18 diffuse Gaussians basis functions placed at the molecular midpoint. The Rydberg orbitals are determined in Improved Virtual Orbital[15] calculations in the field of the $^2\Sigma^+$ ground state of the ion. Rydberg states up to n=8 can be accurately represented. Using the orbitals determined in this procedure, configuration interaction (CI) wave functions for the ion and neutral states are then constructed. The Rydberg states are further optimized in the field of an optical potential due to the dissociating states and the matrix element in (4) is calculated directly from the optimized wave functions. The procedure is outlined below.

For $n^* \gg \ell$, where ℓ is the angular momentum quantum number it can be shown[16] that the matrix element in (4) is given by

$$|\langle \Psi_f|H|\Psi_i^0\rangle|^2 = (1/n^{*3})k\exp(-c/n^*) \tag{5}$$

6

where k and c are constants determined from the calculation of the matrix elements on the left side of (5) for the highest optimized Rydberg states. The high calculated Rydberg states are nearly hydrogenic and the energies can be represented as $E=-(1/2(n^*)^2)$ where $n^*=n-\delta$ and δ is the quantum defect. The density of states can be written as

$$\rho = 1/(E(n^*-1/2) - E(n^*+1/2)) \tag{6}$$

which can be closely represented as

$$\rho = n^{*3}\exp(-1/(2n^{*2})). \tag{7}$$

Substituting (7) and (5) into (4) gives

$$\Gamma = 2\pi k\exp(-(c/n^*)-(.5/n^{*2})). \tag{8}$$

Taking the limit of $n^* \to \infty$ gives the threshold capture width,

$$\Gamma = 2\pi k. \tag{9}$$

The Rydberg wave functions have been refined further by optimizing them in the field of an optical potential due to the Ψ_f states. Feshbach projection operators[17] have been defined which partition the total space such that $\Psi = P\Psi + Q\Psi$ where $P\Psi$ contains the Rydberg states to be optimized and $Q\Psi$ are the Ψ_f states described above. In the usual Feshbach projection operator formalism, an eigenvalue equation is derived for $P\Psi$ that is difficult to solve because it contains an energy-dependent optical potential. However, a new technique[10], based on earlier advances,[18] has been developed in which $P\Psi$

7

can easily be determined by solving the usual CI problem. Writing the total wave function as $\Psi = P\Psi + Q\Psi$, we can write the Schroedinger equation in matrix form as

$$\begin{pmatrix} H_{PP} & H_{PQ} \\ \\ H_{QP} & H_{QQ} \end{pmatrix} \begin{pmatrix} P\Psi \\ \\ Q\Psi \end{pmatrix} = E \; T \begin{pmatrix} P\Psi \\ \\ Q\Psi \end{pmatrix} \tag{10}$$

where $H_{PP} = PHP$, $H_{QP} = QHP$, etc.

Multiplying the matrices in (10) leads to:

$$H_{PP}P\Psi + H_{PQ}Q\Psi = EP\Psi \tag{11}$$

and

$$H_{QP}P\Psi + H_{QQ}Q\Psi = EQ\Psi. \tag{12}$$

From Eq.(12) we have,

$$Q\Psi = H_{QP}P\Psi/(E - H_{QQ}). \tag{13}$$

Substituting Eq.(13) into Eq.(11) leads to a matrix optical potential for $P\Psi$,

$$(H_{PP} + H_{PQ}H_{QP}/(E - H_{QQ})) \; P\Psi = EP\Psi. \tag{14}$$

Since E is on both sides of Eq.(14), it is difficult to solve directly for $P\Psi$. However $P\Psi$ can be easily determined by simply diagonalizing the full H matrix in Eq.(10) and retaining only the coefficients of the $P\Psi$ configurations. In order to divide by $(E - H_{QQ})$ in Eq.(13) and to prevent

8

the mixture of $Q\Psi$ into the $P\Psi$ that is determined by diagonalizing the H

matrix in Eq.(10), it is necessary to first solve for the $Q\Psi$ roots by

diagonalizing H_{QQ}. The low energy $Q\Psi$ roots are then projected out of the H_{QQ}

portion of the H matrix in Eq.(10). $P\Psi$ is then determined by diagonalizing

the transformed H matrix. The free electron is represented by a Rydberg

orbital with a high principal quantum number. Successive $P\Psi$'s are determined

for a series of increasing principal quantum numbers.[30] The widths obtained

by this procedure are then extrapolated to the continuum to yield the

capture width.

These techniques have been tested on the NO molecule and compared to

experimentally derived[19] interaction matrix elements for the B and $L^2\Pi$

repulsive states of NO. These states are known[20] to play an important role

in the DR of the ground state of NO^+. Using the approach outlined above with

a double zeta plus polarization Gaussian basis set and valence CI's of 1335

terms for the entrance channel and 191 terms for the exit channel wave

functions, comparison can be made to the experimental results. The lowest 4

roots in the Q space have been transformed out before solving for the

entrance channel wave functions. The experimentally derived width matrix

elements have been reported only for the lowest (n=3,4) NO $^2\Pi$ Rydberg states

and not for the high (n=7,8) Rydberg states used here for extrapolation to

the continuum. For the $B^2\Pi$ repulsive state Hamiltonian matrix element with

the $3p\pi$ $C^2\Pi$ Rydberg state, the calculated and experimental[6] results are 1229

and 1382.6 cm^{-1}, while for the $4p\pi$ $K^2\Pi$ Rydberg state the results are 714.2

and 803.9 cm^{-1}, respectively. For the $L^2\Pi$ repulsive state, the calculated

and experimental matrix elements with the C state are 546.7 and 549.0 cm^{-1},

respectively. The average difference of only about 8% between theory and

experiment for the lower two levels is quite encouraging, considering that

only small valence space CI wave functions have been used. Since the matrix

9

element must be squared in order to calculate the width, this approach can be expected to yield widths for electron capture to an average accuracy of 17%. Note that this comparison of theory and experiment is only for the n=3,4 Rydberg states for which there are experimental data. Since the n=7,8 Rydberg states are used in the width calculations, an accuracy of better than 17% would be expected. This approach has also been used to calculate widths for the DR of O_2^+ along the $1^1\Pi_g$, $1^3\Pi_g$, $1^3\Sigma_u^-$, $1^1\Sigma_u^+$, and $1^1\Delta_u$ states of O_2 and is described in a reprint and preprint in the Appendix. The widths range from 0.81eV for $^3\Sigma_u^-$ to 0.0022eV for $^3\Pi_g$.

IV. <u>Cross Sections</u>

Under previous AFOSR support the DR cross sections have been calculated using the quantum defect theory expression[21] for DR from ion vibrational level v:

$$\sigma_{DR}^v = (\pi r/2k_e^2)[4\xi_v/(1+\sum_{v'}\xi_{v'})^2] \tag{15}$$

where r is the ratio of multiplicities of the neutral and ion states and k_e is the free electron wave number. The matrix elements ξ_v are given by

$$\xi_v = (\pi/2)[<X_v|\Gamma^{1/2}(R)|X_d>]^2 \tag{16}$$

where X_v and X_d are vibrational wave functions for the ion and dissociative states, respectively. $\Gamma(R)$ is the width, discussed earlier, that connects the electronic continuum of the free electron and ion to the repulsive dissociating resonance state.

10

The denominator in (15) allows for the reduction of the DR cross section due to autoionization, i.e. the emission of the captured electron. The summation over v' in (15) includes all v' that are energetically accessible at a particular electron energy and leads to abrupt decreases in the cross section as new channels open.

A computer program has been written under AFOSR support which uses expression (15) for the calculation of DR cross sections and rates. The program calculates all the required matrix elements using numerically determined vibrational wave functions. The calculation of the cross sections and rates for DR of O_2^+ leading to $O(^1S)$ has been completed and a reprint summarizing the results is included in the Appendix. The calculated DR cross sections for the lowest ten vibrational levels of the ion ground state are shown in Fig. 1. Fig. 1a shows the ion vibrational wave functions, the ion RKR potential curve[8], and the calculated $^1\Sigma_u^+$ dissociative route which is the only route for generating $O(^1S)$ from the lowest ion vibrational levels. Fig.s 1c-k show the large cross section windows. The windows result from the overlap of the nodes in the ion vibrational wave functions with the continuum vibrational wave function in the repulsive state[22]. The number of windows can be predicted by simply counting the number of nodes in the ion vibrational wave function which are at the small internuclear distance side of the intersection of the repulsive curve with the ion vibrational level. The cross sections also show smaller abrupt breaks that arise from autoionization. As the electron energy is increased new ion vibrational levels become accessible and can be populated if autoionization occurs before dissociation, leading to a sudden decrease in the DR cross section at the vibrational level thresholds. The large peak in the v=0 cross section (Fig. 1b) arises from the Franck Condon overlap of the continuum vibrational wave function of the $^1\Sigma_u^+$ state with the peak of the Gaussian like ion wave

11

function for v=0. The calculated rates for DR are discussed further in the Appendix. Comparison of these rates with the calculated and atmospherically derived rates found by other researchers shows that the atmospheric models are observing O_2^+ in a non-Boltzmann vibrational distribution.

The results for generation of $O(^1D)$ are given in a preprint in the Appendix. DR leading to $O(^1D)$ from the lowest two vibrational levels is dominated by the $^3\Sigma_u^-$ and $^1\Delta_u$ states. For the v=2 level, the contribution of $^1\Sigma_u^+$ is of similar importance to that of the other two states. The total rate from v=0 is in agreement with the rate derived from atmospheric models. In contrast to the situation for $O(^1S)$ the rate decreases with increasing vibrational excitation with the rate for v=2 being about one half the rate from v=0.

V. References

1. M. J. Rycroft, Nature 297, 537 (1982); M. Mendillo and J. Baumgardner, Geophys. Res. Lett. 9, 215 (1982).

2. S. L. Guberman, Potential Energy Curves for Dissociative Recombination, in Physics of Ion-Ion and Electron-Ion Collisions ed. by F. Brouillard (Plenum, New York, 1983) pp. 167-200.

3. S. L. Guberman, Int. J. Quantum Chem. Sym. S13, 531 (1979).

4. B. O. Roos, P. R. Taylor, P. E. M. Siegbahn, Chem. Phys. 48, 157(1980).

5. S. Huzinaga, J. Chem. Phys. 42, 1293(1965).

6. T. H. Dunning, Jr., J. Chem. Phys. 55, 716(1971).

7. P. E. M. Siegbahn, J. Chem. Phys. 72, 1647(1980).

8. P. H. Krupenie, J. Phys. Chem. Ref. Data,1, 423(1972).

9. A. C. Allison, S. L. Guberman, and A. Dalgarno, J. Geophys. Res. in press,(1986).

10. S. L. Guberman, to be published.

11. A. Lofthus and P. H. Krupenie, J. Phys. Chem. Ref. Data 6, 113(1977).

12. S. L. Guberman, Nature 327, 408 (1987).

13. S. L. Guberman, The Production of $O(^1D)$ from Dissociative Recombination of O_2^+, Planet. Space Sci., in press, (1988).

14. M. J. Seaton, Rep. Prog. Phys. 46, 167(1983).

15. W. J. Hunt and W. A. Goddard III, Chem. Phys. Lett. 6, 414(1969).

16. S. L. Guberman, Threshold Capture Widths Determined from Bound Rydberg States, ICPEAC Abstracts, (Berlin, 1983), p.286; S. L. Guberman, to be published.

17. H. Feshbach, Ann. Phys. (N. Y.) 5, 357(1958).

18. P. O. Lowdin, in Perturbation Theory and Its Application in Quantum Mechanics, ed. by C. H. Wilcox (John Wiley and Sons, N. Y., 1966), p.255; P. O. Lowdin, Advan. Chem. Phys. 2, 207 (1959); P. O. Lowdin, J. Math. Phys. 3, 969 (1962).

19. R. Gallusser and K. Dressler, J. Chem. Phys. 76, 4311(1982).

20. J. N. Bardsley, Planet. Space Sci. 31, 667(1983).

21. A. Giusti, J. Phys. B $\underline{13}$, 3867(1980).

22. S. L. Guberman, Can. J. Phys. $\underline{64}$, 1621(1986).

VI. Publications

1. S. L. Guberman, Theoretical Studies of Dissociative Recombination, (Invited Paper) in Thermophysical Aspects of Re-entry Flows, ed. by J. N. Moss and C. D. Scott, (American Institute of Aeronautics and Astronautics, New York, 1986) pp.225-242.

2. S. L. Guberman, Windows in Dissociative Recombination Cross Sections, Can. J. Phys. (Invited Paper in Special Issue on Aurora and Airglow Modelling), $\underline{64}$, 1621 (1986).

3. A. C. Allison, S. L. Guberman, and A. Dalgarno, A Model of the Schumann-Runge Continuum of O_2. J Geophys. Res. $\underline{91}$, 10193 (1986).

4. T. L. Kwok, S. L. Guberman, A. Dalgarno, and A. Posen, Dipole Moments and Transition Probabilities of the $a^3\Sigma_g^+ - b^3\Sigma_u^+$ System of Molecular Hydrogen. Phys. Rev., $\underline{34}$, 1962 (1986).

5. A. S.-C. Cheung, K. Yoshino, W. H. Parkinson, S. L. Guberman and D. E. Freeman, Absorption Cross Section Measurements of Oxygen in the Wavelength Region 195-241nm of the Herzberg Continuum, Planet. Space Sci., $\underline{34}$, 1007 (1986).

6. S. L. Guberman, The Production of $O(^1S)$ from the Dissociative Recombination of O_2^+, Nature, $\underline{327}$, 408(1987).

7. S. L. Guberman, The Production of $O(^1D)$ from the Dissociative Recombination of O_2^+, Planet. Space Sci. (Invited Paper for A. Dalgarno

Festschrift Issue) in press (1988).

8. S. L. Guberman, On the Calculation of Threshold Capture Widths from Bound Rydberg States. J. Chem. Phys., to be submitted.

9. S. L. Guberman, The Dissociative Recombination of O_2^+ leading to $O(^1S)$. J. Chem. Phys., to be submitted.

10. S. L. Guberman, The Dissociative Recombination of O_2^+ leading to $O(^1D)$. J. Chem. Phys., to be submitted.

VII. Presentations

1. "Theoretical Studies of Dissociative Recombination,"at the American Institute for Astronautics and Aeronautics 20th Thermophysics Conference, Williamsburg, VA, June, 1985.

2. "$O(^1S)$ From Dissociative Recombination of O_2^+," at the International Association of Geomagnetism and Aeronomy 5th General Assembly, Prague, Czechoslovakia, August 5-17, 1985.

3. "Cross Sections for Dissociative Recombination," American Geophysical Union National Meeting, San Francisco, Dec. 10, 1985.

4. "Theoretical Studies of the Dissociative Recombination of Molecular Ions with Electrons," Department of Physics, University of Massachusetts at Amherst, May 12, 1986.

16

5. "The Dissociative Recombination of O_2^+ with an Electron," American Geophysical Union National Meeting, San Francisco, Dec. 8, 1986.

6. "Theoretical Studies of the Dissociative Recombination of Diatomic Ions with Electrons," International Conference on the Physics of Electronic and Atomic Collisions, Brighton, England, July 24, 1987.
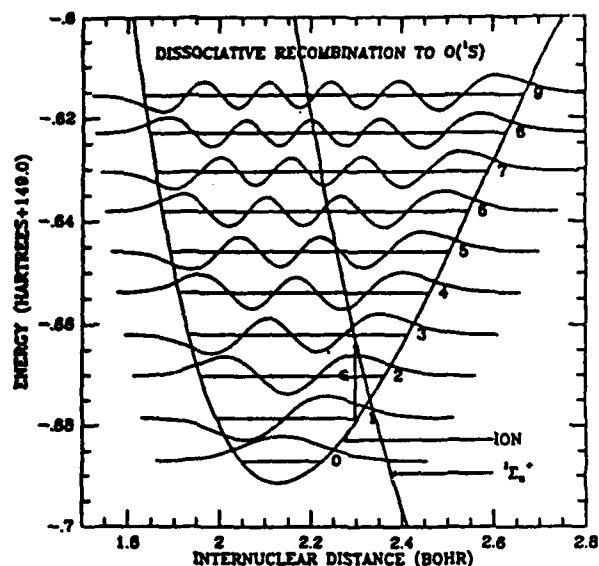
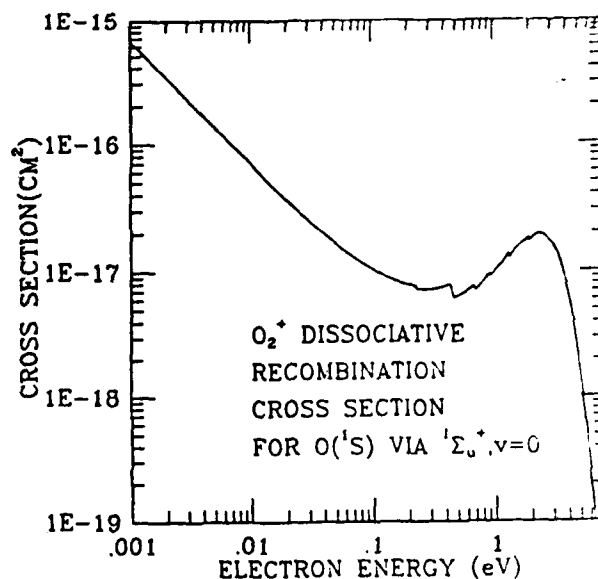Fig. 1a The calculated potential curve for the $^1\Sigma_u^+$ dissociative route and the RKR ion ground state potential curve and vibrational wave functions.

Fig. 1b DR cross section for the v=0 vibrational level of the ion ground state.
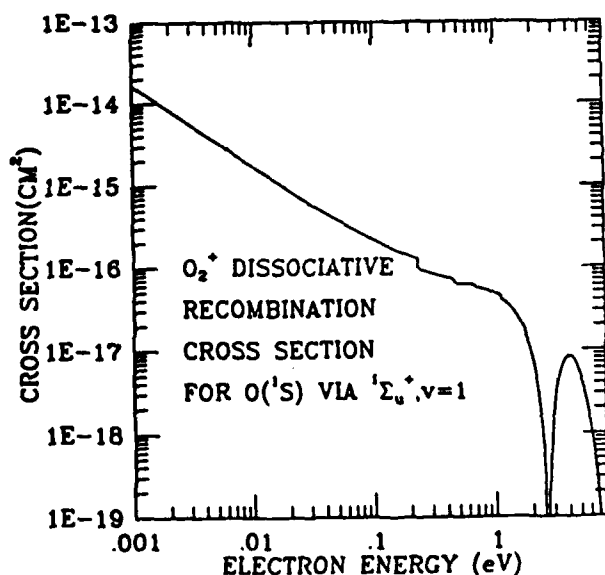
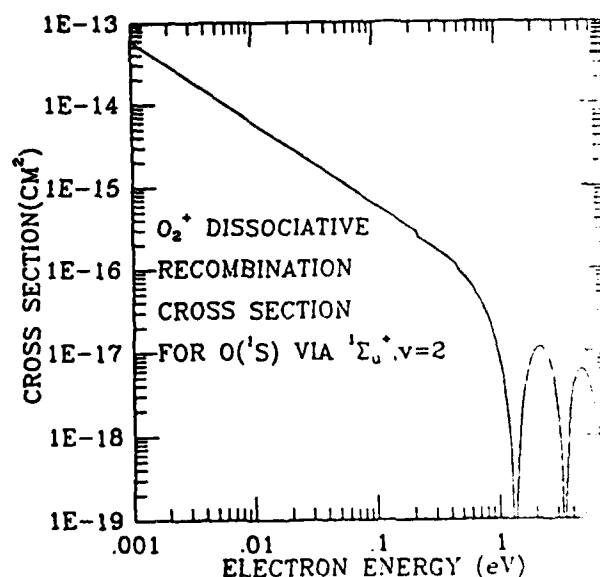Fig. 1c DR cross section for the v=1 vibrational level of the ion ground state.
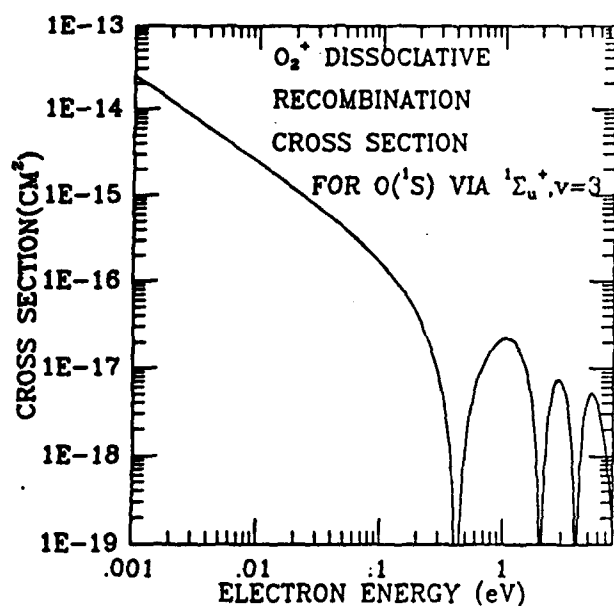
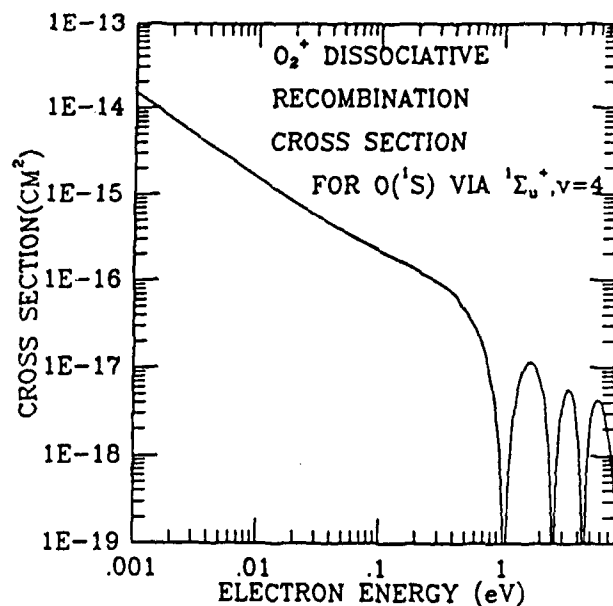Fig. 1d DR cross section from v=2.

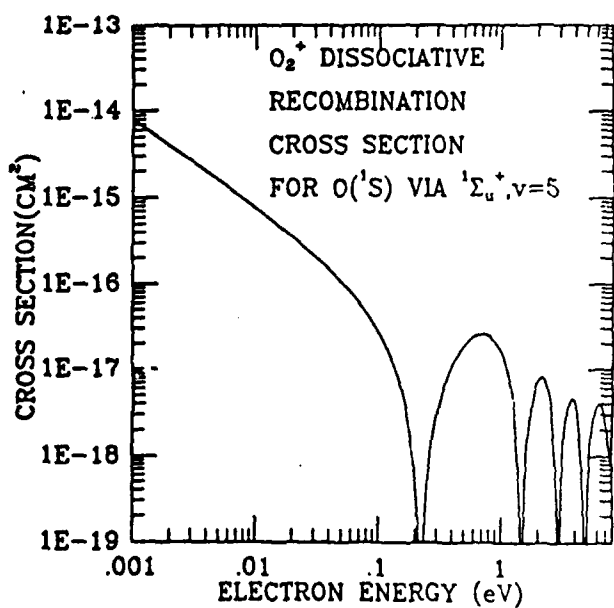Fig. 1e DR cross section from v=3.

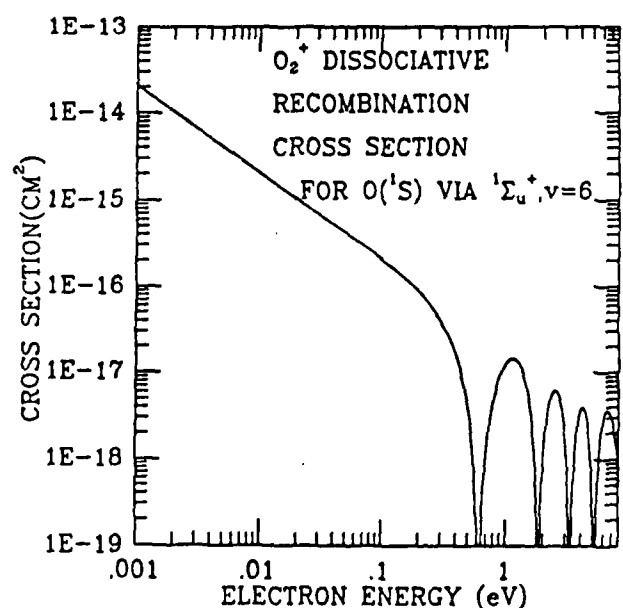Fig. 1f DR cross section from v=4.

Fig. 1g DR cross section from v=5.
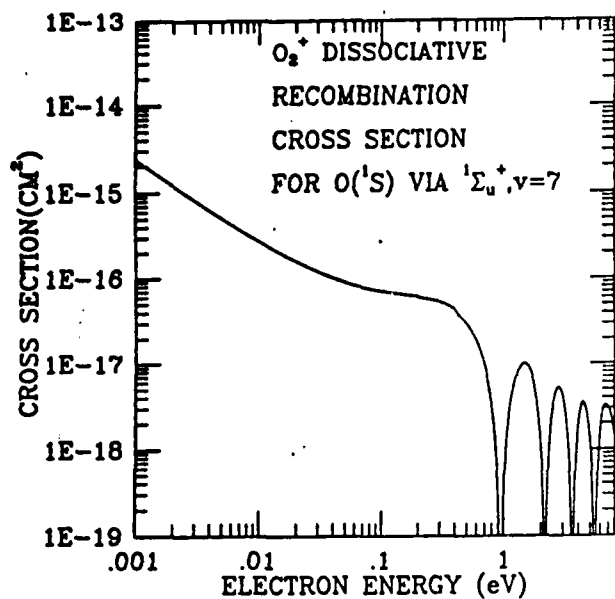
Fig. 1h DR cross section from v=6.

Fig. 1i DR cross section from v=7.
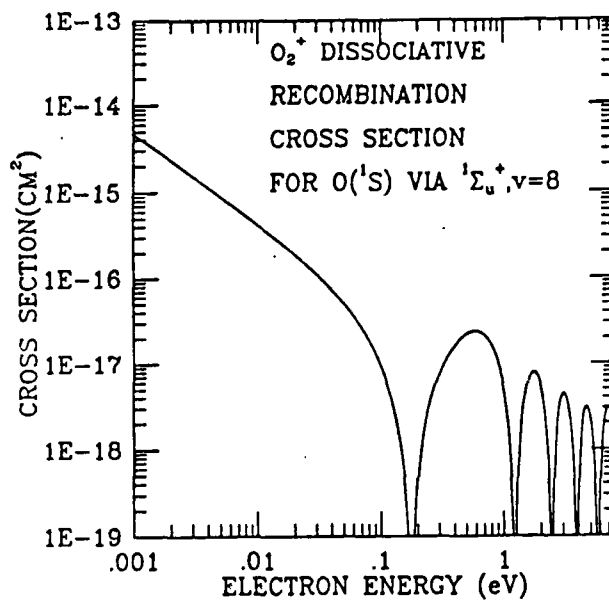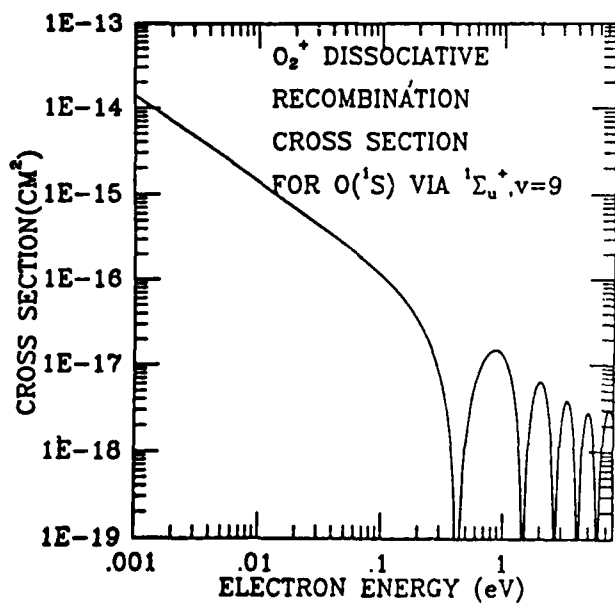

Fig. 1j DR cross section from v=8.

Fig. 1k DR cross section from v=9.

IX. Appendix

1. S. L. Guberman, The Production of $O(^1S)$ from Dissociative Recombination of O_2^+, Nature $\underline{327}$, 498(1987).

2. S. L. Guberman, The Production of $O(^1D)$ from Dissociative Recombination of O_2^+, Planet. Space Sci., in press (1988). Alex Dalgarno Festschrift Issue.

The production of O('S) from dissociative recombination of O₂⁺

Steven L. Guberman

Institute for Scientific Research, 33 Bedford Street, Lexington, Massachusetts 02173, USA and Harvard-Smithsonian Center for Astrophysics, 60 Garden Street, Cambridge, Massachusetts 02138, USA

The suggestion that the dissociative recombination (DR) of O_2^+ with an electron could be an important process in the Earth's upper atmosphere first appeared in the literature over 55 years ago[1]. In 1947, Bates and Massey[2] pointed out that DR of O_2^+ was the only process that could explain the observed electron recombination rates in the E and F1 regions of the ionosphere. In 1954, Nicolet[3] proposed that DR of O_2^+ was the source of the ionospheric emission at 5,577 Å in the Earth's airglow. In the intervening years, the DR of O_2^+ leading to O in the excited 'S state has been the subject of several reviews and many papers[4,5] and has been termed the 'classical'[6] ionospheric source of the well-known green line emission. Nevertheless, the rate coefficient for DR leading to O('S) has never been reliably determined in the laboratory. Here, we report the first theoretical calculations of the rate coefficient for a wide range of temperatures.

The DR of O_2^+ with an electron leading to excited atomic oxygen in the 'S state is described by

$$O_2^+ + e^- \rightarrow O + O(^1S) \tag{1}$$
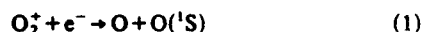
For the low vibrational levels of the ion ($v < 10$), the products of reaction (1) can be described by a single potential energy curve of $^1\Sigma_u^+$ symmetry[7]. In agreement with earlier theoretical studies[7], analyses of the Atmosphere Explorer E satellite measurements have shown a correlation between the quantum yield of O('S) from reaction (1) and the extent of vibrational excitation of the ion although the vibrational distribution was unknown[8]. Dissociation on a surface leading to O('D)+O('S) has been supported by interferometer emission-line profile measurements at 5,577 Å taken by the Dynamics Explorer Satellite[9]. The modelling of this process requires knowledge of the dependence of the DR rate coefficients for production of ground and excited atoms on ion vibrational excitation and electron temperature. Except for the total DR rate coefficient to all channels[10-13], reliable rate coefficients and quantum yields leading to specific excited states of O from individual vibrational levels have not been previously available.

The mechanism[14] for DR is illustrated in Fig. 1. The ion in vibrational level v captures an electron of energy ε into a neutral repulsive state which can dissociate before the captured electron is emitted. The probability of capture into vibrational level v is proportional to a Franck-Condon (FC) factor between a bound ion vibrational wave function and a continuum wave function which has a small internuclear distance (R) turning point near the tip of the vertical arrow in Fig. 1. As ε increases, the turning point of the continuum wave function moves to smaller R, and the FC overlap samples the smaller R region of the bound ion wave function.

The orbitals for the large-scale wave functions reported here for the $^1\Sigma_u^+$ state have been determined in complete active space self-consistent field calculations (CASSCF)[15] over a nuclear-centred contracted gaussian basis set of $6s,3p,2d,1f$ size. The final configuration interaction (CI) wave functions were expanded in terms of the CASSCF orbitals and generated from a ten-term reference set which contained all the configurations needed to describe the dissociation of $^1\Sigma_u^+$ to a 'D and a 'S oxygen atom. The CI involved all single and double excitations to the full virtual space and yielded a 139,946-term wave function. The SWEDEN group of programs (written by C. W. Bauschlicher, P. E. M. Siegbahn, B. Roos, P. Taylor and J. Almhof) and the direct CI method of Siegbahn were used to determine
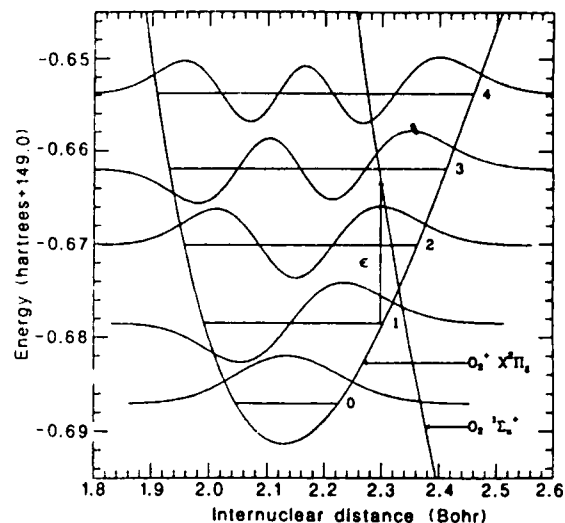

Fig. 1 Potential energy curves for the ground state of O_2^+ (from ref. 18) and for the dissociative $^1\Sigma_u^+$ state calculated here. The ion vibrational wave functions for the lowest five levels are each plotted on the same scale.

the large-scale wave functions[16]. The final energies, corrected for the missing quadruple excitations[17], were determined at 58 points in the range 1.85-8.0 a_0 (Bohr). The resulting potential curve for $^1\Sigma_u^+$ is shown in the region near the ion in Fig. 1. The ground-state ion potential curve is the RKR (Rydberg, Klein, Rees) curve[18] positioned at the experimental ionization potential above the calculated ground state and shifted by 0.0180 a_0 to larger R, to compensate for the difference between the calculated and experimental equilibrium R.

The cross-section, $\sigma(v)$, for DR through ion vibrational level v, was calculated using the expression derived by Giusti[19] in combination with numerically determined vibrational wave functions obtained by solving the one-dimensional nuclear Schrödinger equation in the $^1\Sigma_u^+$ and ion potentials. The cross-section is approximately directly proportional to an electronic width, Γ, which couples the electronic continuum of the free electron and ion to the repulsive dissociating resonance state. The width, a matrix element of the hamiltonian operator, is calculated using Fermi's Golden Rule. High principal quantum number Rydberg orbitals are determined in improved virtual orbital[20] calculations using an extended Rydberg basis set and are used to represent the free electron. The calculation of Γ is then a bound-state problem. The multi-configuration wave function for the ion plus high Rydberg orbital (or free electron) is optimized in the field of an optical potential in a procedure based on the use of Feshbach[21] projection operators (S.L.G., manuscript in preparation). Γ is determined for several values of the principal quantum number, n, of the Rydberg state and a threshold value is determined by extrapolating to $n \rightarrow \infty$. The resulting Γ calculated for the $^1\Sigma_u^+$ state of O_2 is 0.29 eV. The rate coefficient, α, is then obtained by averaging the cross-sections over a Maxwellian distribution of electron energies.

The calculated rate coefficients are shown in Fig. 2. The values of α in the electron temperature (T_e) range $200 < T_e < 400$ K can be closely represented by $\alpha(v=0) = 3.2(+1.6, -1.1) \times 10^{-10} \times (T_e/300)^{-0.34}$, $\alpha(v=1) = 7.5(+1.9, -1.7) \times 10^{-9} \times (T_e/300)^{-0.41}$, $\alpha(v=2) = 2.5(+0.3, -0.4) \times 10^{-8} \times (T_e/300)^{-0.45}$, $\alpha(v=3) = 8.6(+5.6, -4.3) \times 10^{-9} \times (T_e/300)^{-0.60}$ and $\alpha(v=4) = 7.2(+1.4, -2.3) \times 10^{-9} \times (T_e/300)^{-0.36}$. The values for α are for equal ion rotational and electron temperatures. The precision estimates are the average uncertainties that result for an estimated ±15% uncertainty in the electronic width and a ±0.1 eV uncertainty in the position of the dissociative $^1\Sigma_u^+$ route relative to the ion. The $v=0$ level has the lowest α and is a factor of 78 lower than the highest α due to $v=2$. Clearly, for the T_e
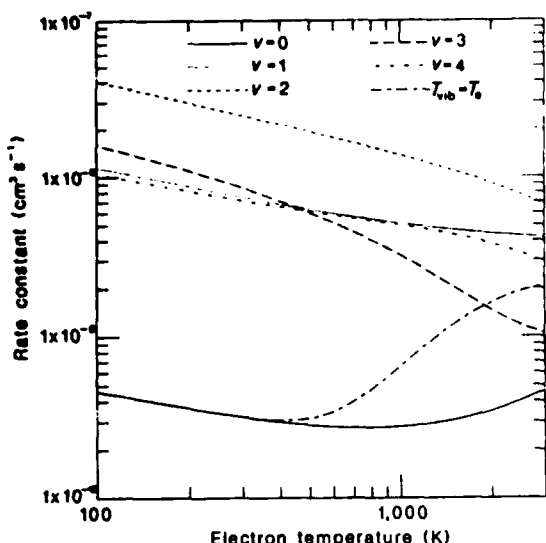
Fig. 2 The calculated rate constant for dissociative recombination along the $^1\Sigma_u^+$ dissociative route for each of the lowest five vibrational levels of the ion and for the case where the vibrational and electron temperatures are identical. In each case, the ion rotational temperature is equal to the electron temperature.

range shown in Fig. 2, the rate coefficient from $v = 2$ is an upper bound to the coefficient at any vibrational temperature, T_{vib}. The relative magnitude of these values can be understood by inspection of Fig. 1. At low electron energies, the FC factor between the continuum vibrational wave function of $^1\Sigma_u^+$ and ion vibrational level v increases with increasing v for $v \leqslant 2$. For $v = 0$, the FC factor increases with electron energy leading to α rising above 790 K. The increase is due to the peak in the cross-section at 1.9 eV which is a 'reflection' of the shape of the $v = 0$ vibrational wave function. Bardsley[22] has shown that a variation of the rate coefficient as $T_e^{-0.5}$ arises if the FC factors are constant with electron energy. For $v = 0, 1, 2, 4$ in the calculations reported here, the FC factors increase as the electron energy increases from zero and the rate coefficients have an exponent which is more positive than -0.5.

Using calculated rates for each of the lowest 10 vibrational levels of the ion, values of α for the equilibrium case in which the electron and vibrational temperatures are identical have been determined and are shown in Fig. 2. For $T < 300$ K, the rate coefficient is indistinguishable in Fig. 2 from the coefficient for $v = 0$. For $T > 300$ K, the α rises due to the increasing contribution of the $v > 0$ rate coefficients to the total rate coefficient and to the increase in the $v = 0$ rate coefficient with increasing T_e. For $800 < T < 1,500$ K, the rate coefficient is closely represented by $\alpha = 8.1 \times 10^{-10} \times (T/1,150)^{1.47}$. It is interesting to note that atmospheric models[4,5,8,9] have all used a negative exponent for the temperature dependence of the rate

coefficient near 1,000 K. The positive exponent obtained here for $T_e = T_{vib}$ near 1,000 K is confirmation that the atmospheric models must be describing conditions for which $T_e \neq T_{vib}$. The most recent atmospheric model[8] reports the rate coefficient to be $(0.83-2.0) \times 10^{-8}$ cm^3 s^{-1} for T_e in the range 680 K–840 K. The results obtained here indicate that the derived atmospheric coefficients must pertain to O_2^+ which cannot be characterized by a Boltzmann temperature but which is instead significantly populated in the $v > 0$ levels.

The above results indicate that a value for the quantum yield of O(^{1}S) is meaningful only if the ion vibrational distribution is specified. Taking the ratio of the DR rate coefficient reported here for $v = 0$ to the laboratory value[10] of the total rate coefficient at $T_e = T_{vib} = 300$ K gives a quantum yield of 0.0016 (+0.0009, -0.0005) for O(^{1}S) from $v = 0$ and should be compared to the original widely used quantum yield of 0.1[23]. The quantum yield reported here supports the more recent view[24] that in the earlier experiment[23] the ions may not have been vibrationally relaxed. However, analysis of the experiments[23,24] is difficult due to the recent measurement[25] of the rapid relaxation of vibrationally excited O_2^+ in an argon buffer. The calculation of the quantum yields from each of the higher vibrational levels is currently in progress.

I thank Dr Richard L. Jaffe for valuable discussions concerning molecular ion rotational considerations. This research is supported at ISR by NASA Ames Cooperative Agreement and at CFA by the NSF and by AFOSR.

Note added in proof: In agreement with the conclusions reported here, a new model of the 5,577 Å emission recorded by the Dynamics Explorer satellite shows that the $v = 1$ and 2 ion vibrational levels are the dominant contributors to O(^{1}S) production[26].

1. Kaplan, J. Phys. Rev. 38, 1048–1051 (1931).
2. Bates, D. R. & Massey, H. S. W. Proc. R. Soc. A192, 1–16 (1947).
3. Nicolet, M. Phys. Rev. 93, 633 (1954).
4. Bates, D. R. in *Applied Atomic Collision Physics* Vol. 1 (eds Massey, H. S. W. & Bates, D. R.) 149–224 (Academic, New York, 1982).
5. Torr, M. R. & Torr, D. G. Rev. Geophys. Space Phys. 20, 91–144 (1982).
6. Vallence Jones, A., Meier, R. R. & Shefov, N. N. J. atmos. terr. Phys. 47, 623–642 (1985).
7. Guberman, S. L. in *Physics of Ion-Ion and Electron-Ion Collisions* 167–200 (Plenum, New York, 1983); Int. J. Quantum Chem. S13, 531–540 (1979).
8. Abreu, V. J., Solomon, S. C., Sharp, W. E. & Hays, P. B. J. geophys. Res. 88, 4140–4144 (1983).
9. Killeen, T. L. & Hays, P. B. J. geophys. Res. 88, 10163–10169 (1983).
10. Alge, E., Adams, N. G. & Smith, D. J. Phys. B16, 1433–1444 (1983).
11. Walls, F. L. & Dunn, G. H. J. geophys. Res. 79, 1911–1915 (1974).
12. Mul, P. M. & McGowan, J. Wm. J. Phys. B12, 1591–1601 (1979).
13. Mehr, F. J. & Biondi, M. A. Phys. Rev. 181, 264–271 (1969).
14. Bates, D. R. Phys. Rev. 78, 492 (1950).
15. Roos, B. O., Taylor, P. R. & Siegbahn, P. E. M. Chem. Phys. 48, 157–173 (1980).
16. Siegbahn, P. E. M., J. chem. Phys. 72, 1647–1656 (1980).
17. Langhoff, S. R. & Davidson, E. R. Int. J. Quantum Chem. 8, 61–72 (1974).
18. Krupenie, P. H. J. Phys. Chem. Ref. Data 1, 423–534 (1972).
19. Giusti, A. J. Phys. B13, 3867–3894 (1980).
20. Hunt, W. J. & Goddard, W. A. III Chem. Phys. Lett. 3, 414–418 (1969).
21. Feshbach, H. Ann. Phys. 5, 357–389 (1958).
22. Bardsley, J. N., J. Phys. B1, 349–364 (1968).
23. Zipf, E. C. Bull. Am. Phys. Soc. 15, 418 (1970).
24. Zipf, E. C., J. geophys. Res. 85, 4232–4236 (1980).
25. Bohringer, H., Durup-Ferguson, M., Fahey, D. W., Fehsenfeld, F. C. & Ferguson, E. E. J. chem. Phys. 79, 4201–4213 (1983).
26. Yee, J.-H. & Killeen, T. L. Planet. Space Sci. 34, 1101–1107 (1986).

The Production of O(^{1}D) From Dissociative Recombination of O$_2^+$

Steven L. Guberman

Institute for Scientific Research
33 Bedford St.
Lexington, MA 02173*

and

Harvard-Smithsonian Center for Astrophysics
60 Garden St.
Cambridge, MA 02138

* Current Address

ABSTRACT—The results of large scale ab initio calculations of the rates for production of $O(^1D)$ by dissociative recombination of O_2^+ are presented for electron temperatures in the range 100-3000K. A $^1\Delta_u$ state is the dominant dissociative route from v=0 and a $^3\Sigma_u^-$ state is the most important route from v=1 and v=2. The calculated total rate for $O(^1D)$ production from v=0 is $2.21(+0.21,-0.24) \times 10^{-7} \times (T_e/300)^{-.46}$ near room temperature. The v=1 and v=2 rates are about 17% and 47% smaller respectively, than the v=0 rate at 300K.

I. Introduction

For the molecular ion, AB^+, dissociative recombination (DR) with an electron is described by

$$AB^+ + e^- \rightarrow A + B \qquad (1)$$
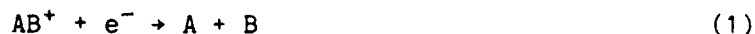
where A or B are ground or excited state atoms or molecular fragments. The study of the process of DR of molecular ions with electrons began with the suggestion of Bates and Massey (1947) that DR could be an important sink for electrons in the ionosphere. It is now recognized that DR can be a rapid process in a wide variety of plasma environments.

Alex Dalgarno has made many significant contributions to the study of DR. These have ranged from fundamental studies of the DR mechanism to applications in interstellar and atmospheric chemistry. The interstellar studies (Dalgarno, 1976, 1982, 1983, 1985, 1986; Dalgarno et al., 1973; Black and Dalgarno, 1977; Dalgarno and Black, 1976) have explored the DR of a wide variety of molecules, ranging in size from H_2^+ to $C_2H_5OH_2^+$. Several of the atmospheric studies of DR (Dalgarno, 1958, 1983) have focused on the role of DR in the production of the red line of atomic O (Dalgarno, 1958; Dalgarno and Walker, 1964; Abreu et al., 1986). Additional contributions relevant to the theory of DR have encompassed the calculation of the energies (Dalgarno and Drake, 1971) and widths (Bransden and Dalgarno, 1952, 1953, 1953a) of autoionizing states and the definition of diabatic states (Dalgarno, 1980). An analysis of the mechanism of DR (Bates and Dalgarno, 1962), based upon the earlier work of Bates (1950, 1950a), provided a number of important insights into DR. Perhaps most relevant to the work presented below was the prediction that the electron temperature dependence of the DR rate coefficient is $T_e^{-0.5}$ unless the curve crossing of the dissociative and molecular ion states leads to a rapid variation of the Franck Condon factors with electron energy.

One of the examples presented by Bates and Dalgarno (1962) was the DR of O_2^+ with an electron, $O_2^+ + e^- \rightarrow O + O$. It is now well recognized that DR of O_2^+ is an important source of $O(^1D)$ in the aurora (Dalgarno and Reid, 1969; Bates, 1982; Rees and Roble, 1986) and airglow (Schaeffer et al., 1972; Bates, 1982; Sharp, 1986).

2

This paper reports the first large scale ab initio calculations of the rate coefficient for generation of $O(^1D)$ atoms from DR of O_2^+ in one of the lowest three vibrational levels. The next section has a discussion of the techniques used to accurately determine the potential curves for the important dissociative routes of O_2. The method used for calculating the cross sections and rates is discussed in Section III. The approach used for determining autoionization widths is summarized in section IV and the resulting rates for $O(^1D)$ production are presented in Section V.

II. Potential Curves

In a seminal paper, Bates (1950a) pointed out that DR rates of significant magnitude at low electron energies require that a repulsive potential curve, describing the motion of the products in (1), crosses the ion curve within the turning points of the ion vibrational level undergoing recombination. Since the time for dissociation can often be rapid compared to the time for emission of the captured electron, the rate of DR can indeed be fast. The process is illustrated in Fig. 1 where an ion in the v=1 vibrational level undergoes DR by capture of an electron of energy ε. For the DR of O_2^+, inspection of the relevant potential curves (Guberman, 1983) shows that for the lowest three vibrational levels of the ion, only five repulsive states can yield $O(^1D)$. The states of interest are the lowest states of $^3\Sigma_u^-$, $^1\Delta_u$, $^1\Sigma_u^+$, $^1\Pi_g$, and $^3\Pi_g$ symmetries. The latter two states do not dissociate adiabatically to ^1D atoms but have avoided crossings with higher states that lead to ^1D atoms. However the two Π states have exceedingly small calculated widths, .0030eV for $^1\Pi_g$ and .0022eV for $^3\Pi_g$ (Guberman, 1987a) at R=2.2819a$_\circ$. These widths are about two orders of magnitude smaller than the smallest width calculated (see Section IV.) for the other three states. Since these small widths will lead to very small DR rates, these states are neglected in the calculation of the total DR rate for production of ^1D atoms. The calculated potential curves for the remaining three states are shown in Fig. 1. The potential curves have been calculated using contracted Gaussian basis sets of [6s,3p,2d,1f] size. The basis sets have been chosen to exclude Rydberg character and the resulting potential curves describe the diabatic valence states needed for DR. The

orbitals are determined separately for each state in Complete Active Space Self-Consistent Field (CASSCF) calculations (Roos et al., 1980) and the Configuration Interaction (CI) wave functions are generated by taking all single and double excitations from a multireference set of configurations to the full virtual orbital space. The direct CI method (Siegbahn, 1980) and the MOLECULE (Almlof)- SWEDEN (Siegbahn et al.) programs were used for the calculation of the potential curves. The CI energies have been corrected for the missing quadruple excitations (Langhoff and Davidson, 1974). The final CI wave functions for the $^3\Sigma_u^-$, $^1\Delta_u$, and $^1\Sigma_u^+$ states had 228,036, 185,400 and 139,946 terms respectively. Further details of the calculations will be reported separately (Guberman, 1987b).

The $^3\Sigma_u^-$ state shown in Fig. 1 intersects the ion at the small R turning point of the v=0 level and is the diabatic continuation of the repulsive wall of the upper state of the well known Schumann-Runge bands. Dissociation along $^3\Sigma_u^-$ after capture by a zero energy electron from v=0 leads to a ground state atom and a ^1D atom, each with 2.5 eV kinetic energy. Dissociation along the $^1\Delta_u$ route from v=0 leads to two ^1D atoms, each with 1.5eV kinetic energy. Dissociation along $^1\Sigma_u^+$ leads to a ^1S and a ^1D atom, each with 0.4 eV kinetic energy from v=0.

III. Methods for Cross Sections and Rates

The cross sections, σ_v, for direct DR (Bardsley, 1968) from ion vibrational level v have been calculated using the expression derived by Giusti (1980) from quantum defect theory for the case of a single dissociative state and many open ion vibrational levels, v',

$$\sigma_v = (\pi r / 2k_e^2)[4\xi_v/(1+\textstyle\sum_{v'}\xi_{v'})^2] \tag{2}$$

where $k_e^2 = 2m\epsilon$, k_e is the wave number of the incident electron, m is the electron mass, and r the ratio of multiplicities of the neutral and ion states. The matrix elements ξ_v are given by

4

$$\xi_v = (\pi/2)[\langle X_v | \Gamma^{1/2}(R) | X_d \rangle]^2 \qquad (3)$$

where X_v and X_d are vibrational wave functions for the ion and dissociative states, respectively. The integration in (3) is over both R and the electronic coordinates. The vibrational wave functions are determined by the Numerov method on a $0.001a_0$ grid between 0.0 and $8.0a_0$. The integration over R in (3) is done by Simpson's rule. The width, $\Gamma(R)$, connects the electronic continuum of the free electron and ion to the repulsive dissociating resonance state and is given by the Golden Rule,

$$\Gamma(R) = 2\pi \langle \{\Phi_{ion}(x,R)\phi_\varepsilon(x,R)\} | H | \Phi_d(x,R) \rangle^2. \qquad (4)$$

In (4) H is the Hamiltonian, the integration is over the electronic coordinates represented by x, and the wave functions from left to right in (4) are for the ion core, the free electron, and the dissociative neutral state. The antisymmetrized product of the ion core and free electron wave functions is denoted by $\{\}$.

The indirect DR process (Bardsley, 1968a; Giusti, 1980; Giusti-Suzor et al., 1983) in which recombination occurs into a vibrationally excited Rydberg state which is predissociated by the repulsive routes discussed here, has not been included in the cross section calculations. The indirect process is not expected to be a significant contributor to $O(^1D)$ production.

Rate constants have been calculated by averaging the calculated cross sections over a Maxwellian distribution of electron energies.

IV. Electronic Widths

The widths given in Eq. (4) have been calculated by using high Rydberg orbitals to represent the free electron (Guberman, 1986, 1987a). Since all the orbital amplitudes in (4), except for that of the free electron, fall off rapidly with increasing x, only the free electron amplitude near the nuclei is needed for the width calculation. Except for a normalization factor, high Rydberg orbitals have a shape similar to free electron orbitals near the nuclei. A density of states is then inserted into (4) for the normalization (Guberman, 1987a). The Rydberg orbitals are calculated using the Improved

5

Virtual Orbital (IVO) method (Hunt et al., 1969) in a basis set of 18 diffuse
Gaussians positioned midway between the nuclei (Guberman, 1987a). Each Rydberg
orbital is an eigenfunction of an IVO Hamiltonian which is unique for each
molecular symmetry.

The wave function of the ion plus a free electron in (4) is represented by
antisymmetrized products of a valence CI description of the ground state of O_2^+
with the Rydberg orbital and with the valence virtual orbitals of the same
symmetry as the Rydberg orbital. For the width calculations, the dissociative
states were represented by full valence CI wave functions in which excitations
out of the 2σ orbitals were included. For $^3\Sigma_u^-$ this procedure leads to a 48
term CI wave function for the dissociative state and a 954 term CI wave
function for the entrance channel. For $^1\Delta_u$ and $^1\Sigma_u^+$, the entrance and exit
channel wave functions have 42 and 630 terms respectively. The size of the
entrance channel wave function is increased further by allowing the entrance
channel to mix in higher nonphysical routes from the exit channel. A Feshbach
(1958) projection operator procedure has been used to implement this procedure
(Guberman, 1986, 1987a).

The entire procedure is repeated for several values of the Rydberg orbital
principal quantum number with the highest accurately determined orbital having
$n=8$. The widths calculated from each value of n are then extrapolated to the
continuum. A comparison to experimentally derived (Galluser et al., 1982)
predissociation matrix elements for NO indicates that the widths calculated by
this procedure deviate from experiment by about 15%.

For $^3\Sigma_u^-$, the calculated width is 0.81 eV near $R=2.08a_0$ and decreases to
0.54eV at $1.78a_0$. For $^1\Delta_u$ and $^1\Sigma_u^+$, the width is relatively constant with R,
having a value of 0.44eV and 0.29eV respectively at $R=2.28a_0$,varying by only
about 2% over the region of significant nuclear overlap with the $v=0,1,2$ ion
wave functions. Since the estimated uncertainty in the calculated widths is
15%, the variation of the width with R has been ignored for $^1\Delta_u$ and $^1\Sigma_u^+$ but
has been accounted for in expression (3) for $^3\Sigma_u^-$ (S. L. Guberman, 1987b).

V. Calculated DR Rates

The calculated rate constants for the three dissociative routes discussed

here are shown in Fig.s 2, 3, and 4 for each of the lowest three vibrational levels of the nonrotating ion. For $200 \leq T_e \leq 400K$, the DR rates are given in Table 1. The uncertainties in the rates are average uncertainties computed from an estimated ±15% uncertainty in the calculated widths and an estimated ±0.1eV uncertainty in the position of the potential curves relative to the ion curve. The highest DR rates are from $^3\Sigma_u^-$. However, for v=0, the rate along $^1\Delta_u$ is more than half the DR rate along $^3\Sigma_u^-$. Since $^1\Delta_u$ leads to two ^1D atoms, the highest rates for producing ^1D atoms from v=0 are from $^1\Delta_u$. However, from v=1 and v=2 (Fig.s 2-4), the highest rates for $O(^1D)$ production are from $^3\Sigma_u^-$.

As pointed out by Bates and Dalgarno(1962), the temperature dependence of the direct DR process will vary as $T_e^{-0.5}$ if the amplitude of the ion wave function does not vary substantially over the range of electron energies of interest. Such a situation can arise for any ion wave function if the dissociative curve is very steep. In general, an intersection of the dissociative route with the ion vibrational level near the peak of the ion wave function will lead to slowly varying nuclear overlap terms and electron temperature dependencies near -0.5, while intersection at a point where the absolute value of the ion wave function amplitude is increasing (decreasing) will usually lead to temperature dependencies more positive (negative) than - 0.5. Note that the denominator in (2) has a tempering effect upon these conclusions. Two such cases are illustrated in Cases a and b of Fig. 2 of Bates and Dalgarno (1962). The latter Case shows a dissociative route intersecting the v=0 level in the nonclassical region on the large R side of the ion equilibrium internuclear distance and resembles the situation found here for $^1\Sigma_u^+$.

For $^1\Sigma_u^+$, the amplitudes of the ion wave functions at low electron energies increase most rapidly for v=0. The increase for v=1 is less rapid than for v=0. For v=2, the intersection is near the outer peak in the v=2 wave function. The calculated temperature dependencies given in Table 1 for $^1\Sigma_u^+$ show the predicted pattern. The most positive exponent is for v=0 followed by v=1 and v=2. For the other two dissociative routes the exponents are near 0.5 for v=0 since the intersections with the ion are within the classical turning points and the amplitude is changing slowly. For v=1 and 2 and $^3\Sigma_u^-$ and $^1\Delta_u$, one must take into account the overlap of the nodes in the ion wave functions with the nodes in the continuum wave functions. The exponents are difficult to

7

predict in these cases by visual inspection of Fig.1.

Also shown in Fig.s 2-4 are the rates for the equilibrium case where the vibrational temperature is set equal to the electron temperature. For $^3\Sigma_u^-$, the equilibrium case rates are nearly indistinguishable from the v=0 rates over the span of electron temperatures plotted. For $^1\Delta_u$, the equilibrium rates fall below the v=0 rates at high electron temperatures. For $^1\Sigma_u^+$, the equilibrium rates increase dramatically above 450K, since the rates for v=1 and v=2 are substantially larger than for v=0 (Guberman, 1987).

It is interesting to examine the ^1D production in each channel as a function of ion vibrational level. From v=0, 56% of the ^1D atoms arise from the $^1\Delta_u$ channel and 44% arise from the $^3\Sigma_u^-$ channel. For v=1, 58% of the ^1D atoms are in the $^3\Sigma_u^-$ channel and 4% appear in the $^1\Sigma_u^+$ channel with 0.52eV kinetic energy. For v=2, 45% of the atoms are in the 2.7eV $^3\Sigma_u^-$ channel and 21% are in the 0.64eV $^1\Sigma_u^+$ channel. Each vibrational level will lead to a unique three component Doppler line shape. From these data, the vibrational distribution of the recombining ion could be determined in an experiment that accurately determines the Doppler widths of the radiating ^1D atoms.

The total rate for producing ^1D atoms for T_e in the above range from v=0 (Table 1) is $2.21(+0.21,-0.24) \times 10^{-7} \times (T_e/300)^{-0.46} cm^3/sec$ and is in good agreement with the value originally reported by Zipf (1970) of 1.9×10^{-7} cm^3/sec. Note that the total calculated rate decreases with increasing v. The rate from v=2 is about half the rate from v=0. The variation of the rate with v contrasts sharply to that for producing $O(^1S)$ (Guberman, 1987) shown in the fourth column of Table 1 and Fig. 4. The rotationless $O(^1S)$ rate for v=2 is a factor of 80 larger than the rate from v=0. The total calculated rate up to T_e=3000K for ^1D production is shown in Fig. 5. Rates for both J=0 and rotationally averaged rates in which the rotational temperature is the same as T_e are shown. Clearly, accounting for the rotational temperature has only a slight effect upon the calculated rates. The rotationally averaged and the rotationless results from v=0 and for the case of equal vibrational and electron temperatures are each superimposed on the scale of Fig. 5.

There have been several aeronomic determinations of the ^1D production rate by DR. The literature prior to 1982 has been reviewed by M. R. Torr and D. G. Torr (1982). Among the deduced production rates are $(2.1\pm0.48)\times10^{-7}\times$ $(T_e/300)^{-0.85}$ (P. B. Hays et al, 1978; R. Link et al., 1981) and

8

$(1.96\pm0.67)\times10^{-7}\times(T_e/300)^{-.55}$ (Abreu et al., 1983). These rates were obtained by combining the total rate found by Walls and Dunn (1974) and Torr et al. (1976) with a model determination of the ^1D quantum yield. A recent determination (Abreu et al., 1986) which improves the models by including quenching of $O(^1D)$ by $O(^3P)$ leads to a rate of $1.9\times10^{-7}\times(T_e/300)^{-.55}$. The deduced rates are in excellent agreement with the v=0 rate calculated here at room temperature. The atmospheric quantum yields are derived at ionospheric temperatures. At $T_e=760K$, the ^1D production rate calculated here is $1.41(+0.14,-0.16)\times10^{-7}$ compared to the model rate (Abreu et al., 1986) of 1.14×10^{-7}. Considering the likely precision on the latter rate, the rates reported here are in agreement with the model rates. Note that the precision on the rates calculated here do not exclude the possibility that the models apply to vibrationally excited O_2^+.

None of the above models have included ^1D production due to cascade from ^1S. The DR contribution to cascade will be unimportant if the ion is mostly in v=0 but should be considered if a substantial fraction of the ions are vibrationally excited.

VI. Conclusions

Three neutral dissociative states of $^3\Sigma_u^-$, $^1\Delta_u$, and $^1\Sigma_u^+$ symmetries have been identified as the major sources of $O(^1D)$ from DR of the lowest three vibrational levels of O_2^+. DR rates along each of these routes have been calculated for electron temperatures in the range 100-3000K. The total rate for generating DR from v=0, $2.21(+0.21,-0.24)\times10^{-7}\times(T_e/300)^{-0.46}cm^3/sec$, agrees with prior rates determined from aeronomic models and laboratory measurements. However, the variation of the rate with v and the precision on the calculated rates leaves room for the possibility that the atmospheric models and the laboratory experiments could be observing vibrationally excited ions. The total rate for generating $O(^1D)$ decreases with increasing v in contrast to the rates for generating $O(^1S)$ which increase markedly with increasing v.

Acknowledgments

REFERENCES

Abreu, V. J., Solomon, S. C., Sharp, W. E., Hays, P. B. (1983) The Dissociative Recombination of O_2^+: The Quantum Yield of $O(^1S)$ and $O(^1D)$. J. Geophys. Res. **88**, 4140.

Abreu, V. J., Yee, J. H., Solomon, S. C. and Dalgarno, A. (1986) The Quenching Rate of $O(^1D)$ by $O(^3P)$. Planet. Space Sci. **34**, 1143.

Almlof, J., MOLECULE, a Gaussian integral program.

Bardsley, J. N. (1968) Configuration interaction in the continuum states of molecules. J. Phys. B **1**, 349.

Bardsley, J. N. (1968a) The theory of dissociative recombination. J. Phys. B **1**, 365.

Bates, D. R. (1950) Electron Recombination in Helium. Phys. Rev. **77**, 718.

Bates, D. R. (1950a) Dissociative Recombination. Phys. Rev. **78**, 492.

Bates, D. R. (1982) Airglow and Auroras, in Applied Atomic Collision Physics, (Edited by Massey, H. S. W. and Bates, D. R.) pp. 149-224. Academic Press, New York.

Bates, D. R. and Dalgarno, A. (1962) Electronic Recombination, in Atomic and Molecular Processes, (Edited by Bates, D. R.) pp. 245-271. Academic Press, New York.

Bates, D. R. and Massey, H. S. W. (1947) The basic reactions in the upper atmosphere II. The theory of recombination in the ionized layers. Proc. Roy. Soc. **192**, 1.

Black, J. H. and Dalgarno, A. (1977) Models of the Interstellar Clouds. I. The Zeta Ophiuchi Cloud. Ap. J. Suppl. **34**, 405.

11

Bransden, B. H. and Dalgarno, A. (1952) A Variational Method for Radiationless Transitions. Phys. Rev. **88**, 148.

Bransden, B. H. and Dalgarno, A. (1953) The Calculation of Autoionization Probabilities -I. Perturbation Methods with Application to Autoionization in Helium. Proc. Phys. Soc. **A66**, 904.

Bransden, B. H. and Dalgarno, A. (1953a) The Calculation of Autoionization Probabilities -II: A Variational Method for Radiationless Transitions with Application to the $(2s)^2$ $^1S-(1sks)^1S$ Transition of Helium. Proc. Phys. Soc. **A66**, 911.

Dalgarno, A. (1958) The Altitudes and Excitation Mechanisms of the Night Airglow. Annales de Geophysique **14**, 241.

Dalgarno, A. (1976) The interstellar molecules CH and CH^+, in Atomic Processes and Applications (Edited by Burke, P. G. and Moiseiwitsch, B. L.)pp.109-132, North-Holland Publishing Co.

Dalgarno, A. (1980) Diabatic and Resonance Molecular States. Physica Scripta **21**, 492.

Dalgarno, A. (1982) Molecules in Interstellar Space, in Applied Atomic Collision Physics (Edited by Massey, H. S. W. and Bates, D. R.), pp. 427-467. Academic Press, New York.

Dalgarno, A. (1983) Electron-Ion and Proton-Ion Collisions in Astrophysics, in Physics of Ion-Ion and Electron-Ion Collisions, (Edited by Brouillard, F. and McGowan, J. W.), pp.1-36. Plenum Press, New York.

Dalgarno, A. (1985) Molecular Astrophysics, in Molecular Astrophysics, (Edited by Diercksen, G. H. F. et al.), pp.3-22. D. Reidel, Dordrecht.

Dalgarno, A. (1986) Is Interstellar Chemistry Useful? Q. Jl. R. astr. Soc. 27,

83.

Dalgarno A. and Black, J. H. (1976) Molecule formation in the interstellar gas. Rep. Prog. Phys. **39**, 573.

Dalgarno, A. and Drake, G. W. F. (1971) An Energy Maximization Method for Autoionizing States. Chem. Phys. Letters **11**, 509.

Dalgarno, A., Oppenheimer, M., and Berry, R. S. (1973) Chemiionization in Interstellar Clouds. Ap. J. **183**, L21.

Dalgarno A. and Reid, R. H. G. (1969) Excitation of Forbidden Lines by Dissociative Recombination. Mem. Soc. Roy. Sci. Liege **17**, 157.

Dalgarno, A. and Walker, J. C. G. (1964) The Red Line of Atomic O in the Day Airglow. J. Atmos. Sci. **21**, 463.

Feshbach, H. (1958) Unified Theory of Nuclear Reactions. Ann. Phys. (N.Y.) **5**, 357.

Galluser, R. and Dressler, K. (1982) Multistate Vibronic Coupling between the Excited $^2\Pi$ states of the NO Molecule. J. Chem. Phys. **76**, 4311.

Giusti, A. (1980) A multichannel quantum defect theory approach to dissociative recombination. J. Phys. B **13**, 3867.

Giusti-Suzor, A., Bardsley, J. N., and Derkits, C. (1983) Dissociative recombination in low-energy e-H_2^+ collisions. Phys. Rev. A **28**, 682.

Guberman, S. L. (1983) Potential Energy Curves for Dissociative Recombination, in Physics of Ion-Ion and Electron-Ion Collisions (Edited by Brouillard, F. and McGowan, J. W.), pp. 167-200. Plenum Press, New York.

Guberman, S. L. (1986) Theoretical Studies of Dissociative Recombination, in Thermophysical Aspects of Re-entry Flows (Edited by Moss, J. N. and Scott, C.

D.) pp. 225-242. AIAA, New York.

Guberman, S. L. (1986a) Windows in direct dissociative recombination cross
sections. Can. J. Phys. **64**, 1621.

Guberman S. L. (1987) The production of $O(^1S)$ from dissociative recombination
of O_2^+, Nature **327**, 408.

Guberman, S. L. (1987a) A Bound State Approach for Calculating Resonance
Widths. In preparation.

Guberman, S. L. (1987b) to be published.

Hays, P. B., Rusch, D. W., Roble, R. G. and Walker, J. C. G. (1978) The
OI(6300A) Airglow. Rev. Geophys. Space Phys. **16**, 225.

Hunt, W. J. and Goddard III, W. A. (1969) Excited States of H_2O Using Improved
Virtual Orbitals. Chem. Phys. Lett. **3**, 414.

Langhoff, S. R. and Davidson, E. R. (1974) Int. J. Quant. Chem. **8**, 61.

Link, R., McConnell, J. C. and Shepherd, G. G. (1981) A Self-Consistent
Evaluation of the Rate Constant for the Production of the OI6300A Airglow.
Planet. Space Sci. **29**, 589.

Rees, M. H. and Roble, R. G. (1986) Excitation of $O(^1D)$ atoms in aurorae and
emission of the OI 6300A line. Can. J. Phys. **64**, 1608.

Roos, B. O., Taylor, P. R. and Siegbahn, P. E. M. (1980) A Complete Active
Space SCF Method (CASSCF) using a Density Matrix Formulated Super-CI
Approach. Chem. Phys. **48**, 157.

Schaeffer, R. C., Feldman, P. D. and Zipf, E. C. (1972) Dayglow [OI] 6300 and
5577 A Lines in the Early Morning Ionosphere. J. Geophys. Res. **77**, 6828.

Sharp, W. E. (1986) Sources of the emission features between 2000 and 8000A in the thermosphere. Can. J. Phys. **64**, 1594.

Siegbahn, P. E. M. (1980) Generalizations of the direct CI method based on the graphical unitary approach. II Single and double replacements from any set of reference configurations. J. Chem. Phys. **72**, 1647.

Siegbahn, P. E. M., Bauschlicher, C. W., Roos, B., Heiberg, A., Taylor, P. R. and Almlof, J., SWEDEN, a vectorized SCF-MCSCF-direct CI program.

Torr, M. R. and Torr, D. G. (1982) The Role of Metastable Species in the Thermosphere. Rev. Geophys. Space Phys. **20**, 91.

Torr, D. G., Torr, M. R., Walker, J. C. G., Nier, A. O., Brace, L. H., and Brinton, H. C. (1976) Recombination of O_2^+ in the Ionosphere. J. Geophys. Res. **81**, 5578.

Zipf, E. C. (1970) The Dissociative Recombination of O_2^+ into Specifically Identified Final Atomic States. Bull. Am. Phys. Soc. **15**, 418.
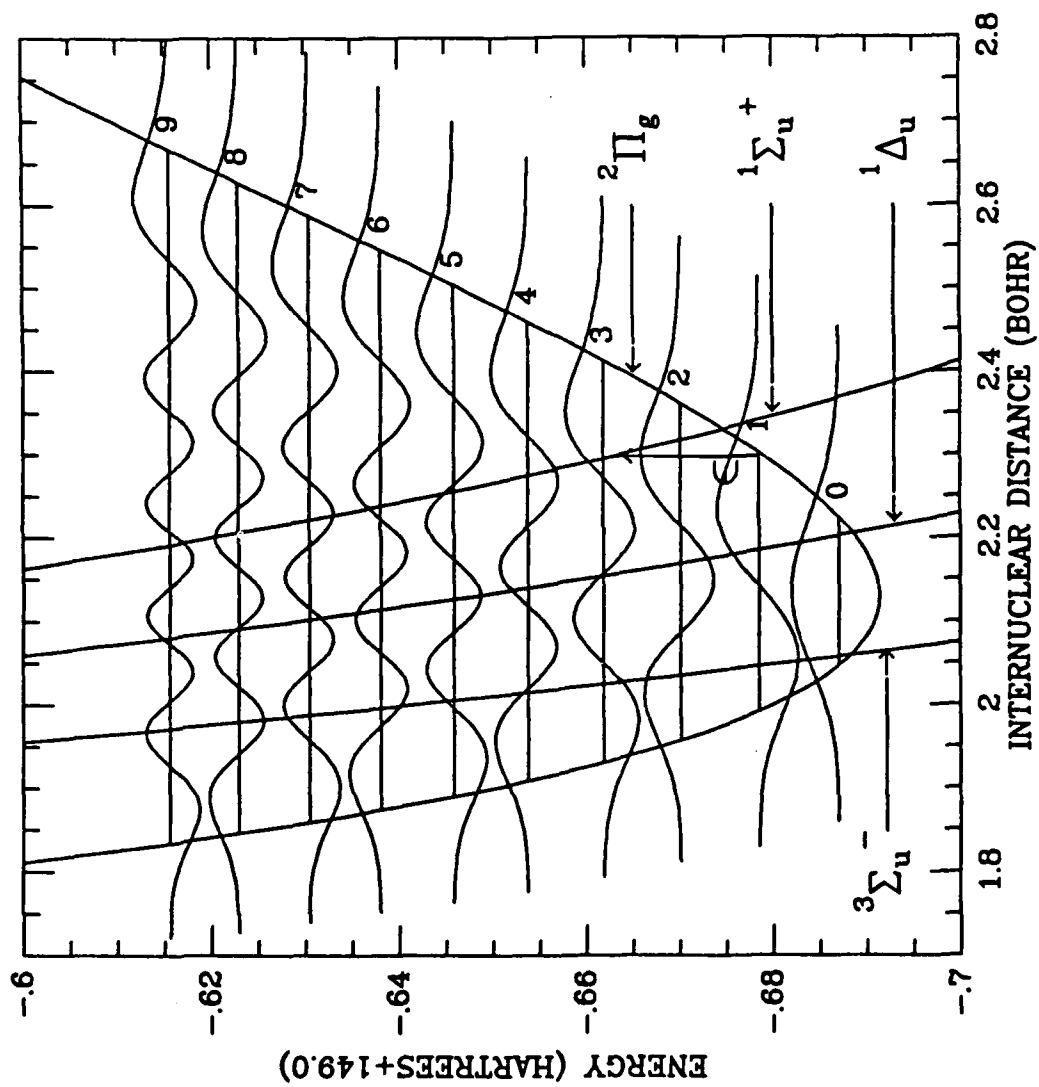
TABLE 1. Dissociative recombination rates along three channels for each of the lowest three vibrational levels of the ion at 200K≤T_e≤400K and J=0.*
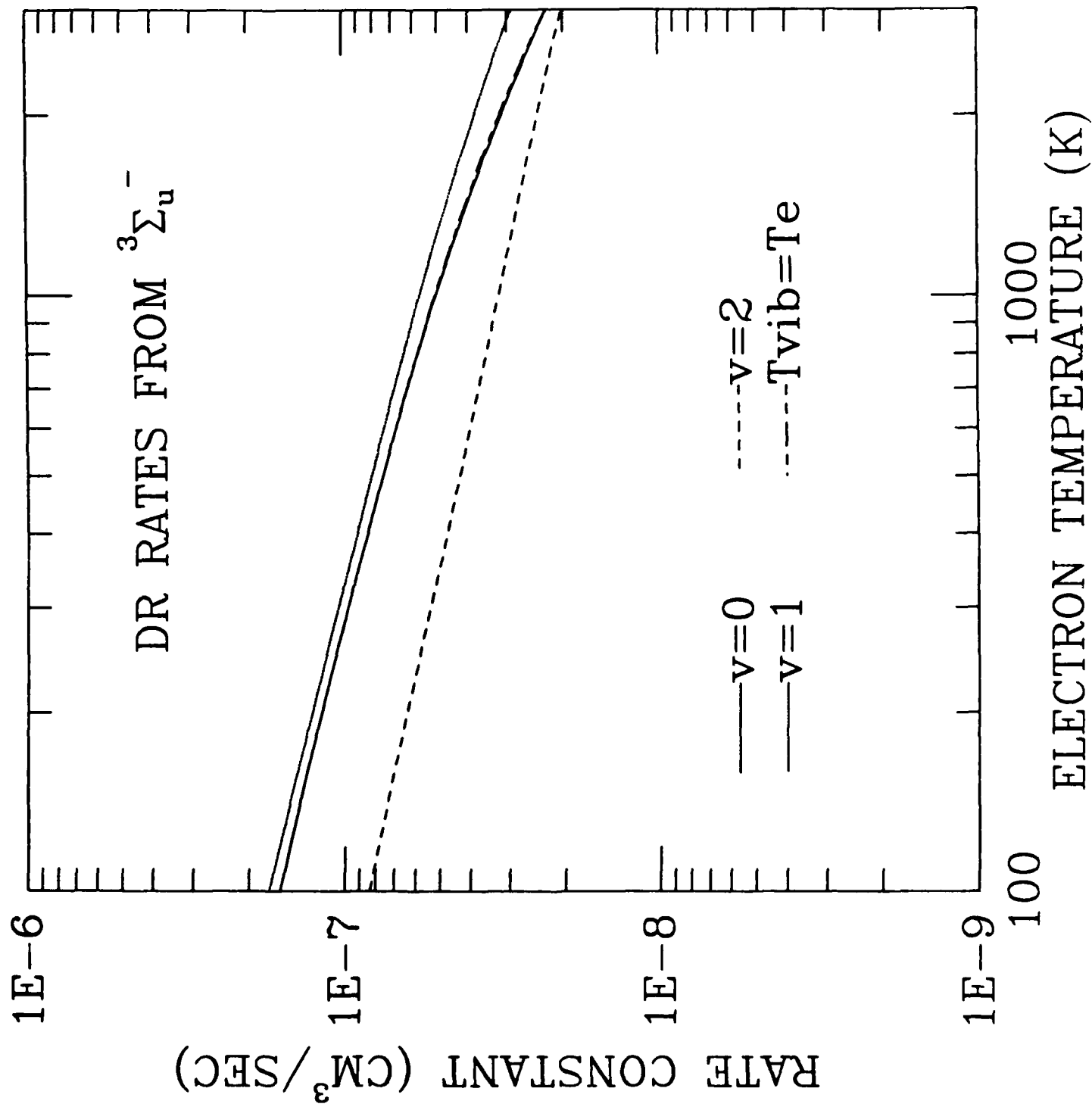
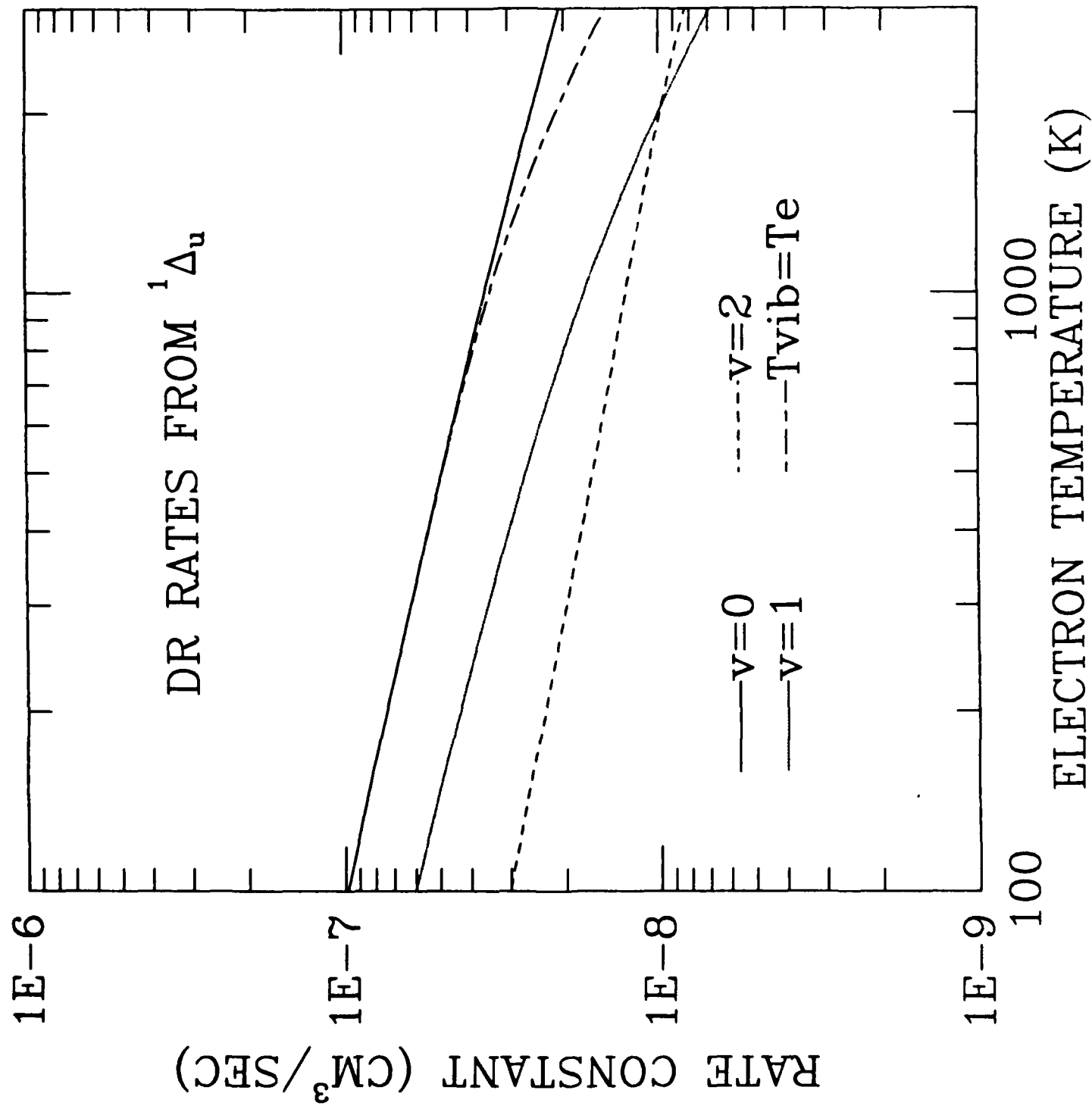| v	$^3\Sigma_u^-$	$^1\Delta_u$	$^1\Sigma_u^+$	Total ^{1}D Production Rate
0	0.97(+0.09,-0.10)[0.48]	0.62(+0.06,-0.07)[0.45]	0.0030(+0.0016,-0.0011)[0.34]	2.21(+0.21,-0.24)[0.46]
1	1.05(+0.05,-0.07)[0.47]	0.35(+0.06,-0.07)[0.52]	0.073(+0.019,-0.017)[0.41]	1.82(+0.19,-0.23)[0.49]
2	0.53(+0.06,-0.08)[0.42]	0.20(+0.05,-0.06)[0.39]	0.24(+0.03,-0.04)[0.45]	1.17(+0.19,-0.24)[0.42]

*All rates are total recombination rates except for the last column which is the rate for production of ^{1}D atoms. The rates in the last column are obtained by adding columns 2 and 4 to twice column 3. The electron temperature dependence is shown in square brackets following each rate. Each rate is multiplied by 10^{+7}. The rate for $^3\Sigma_u^-$ from v=0 is read as $0.97(+0.09,-0.10) \times 10^{-7} \times (T_e/300)^{-0.48}$.
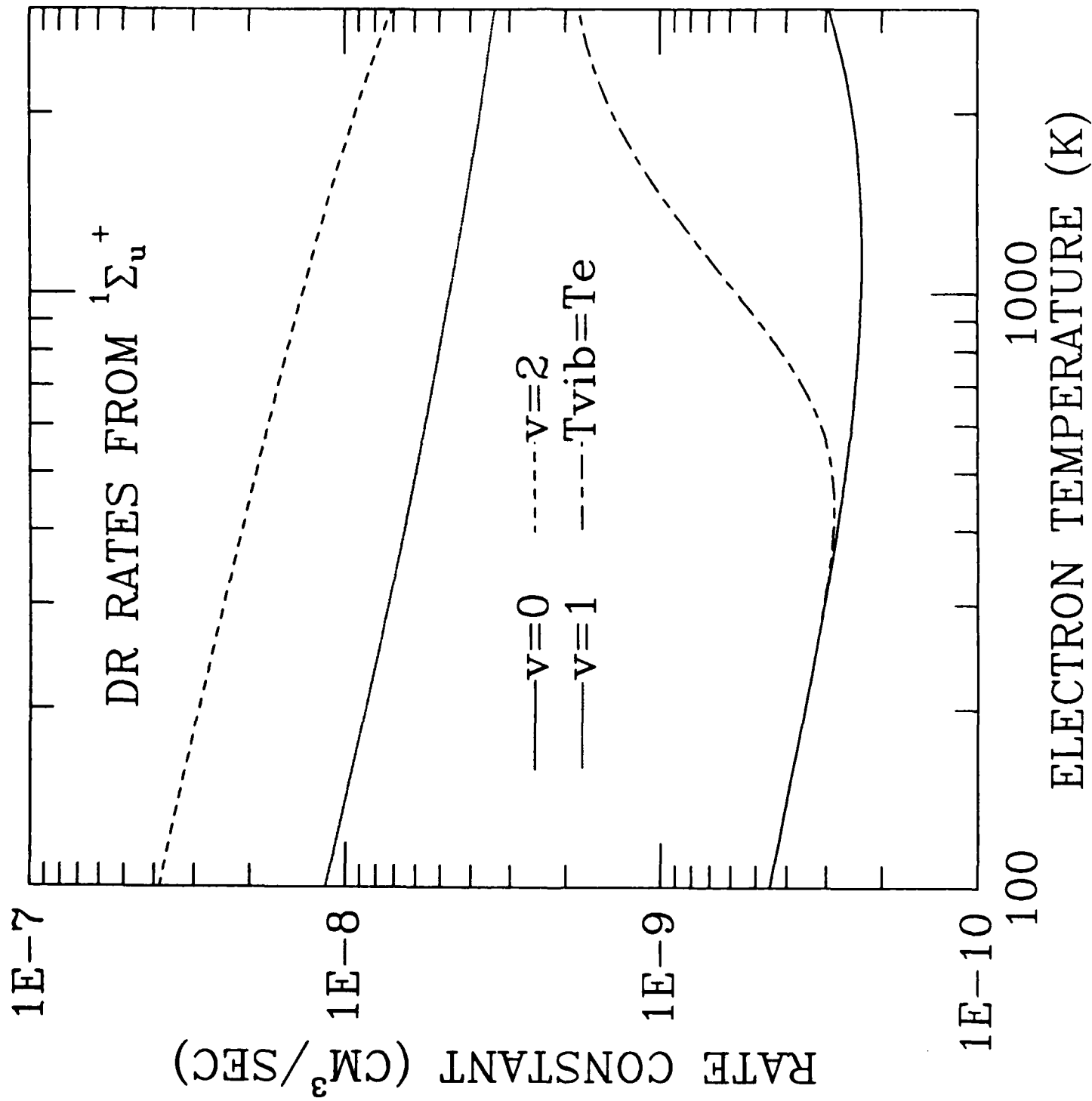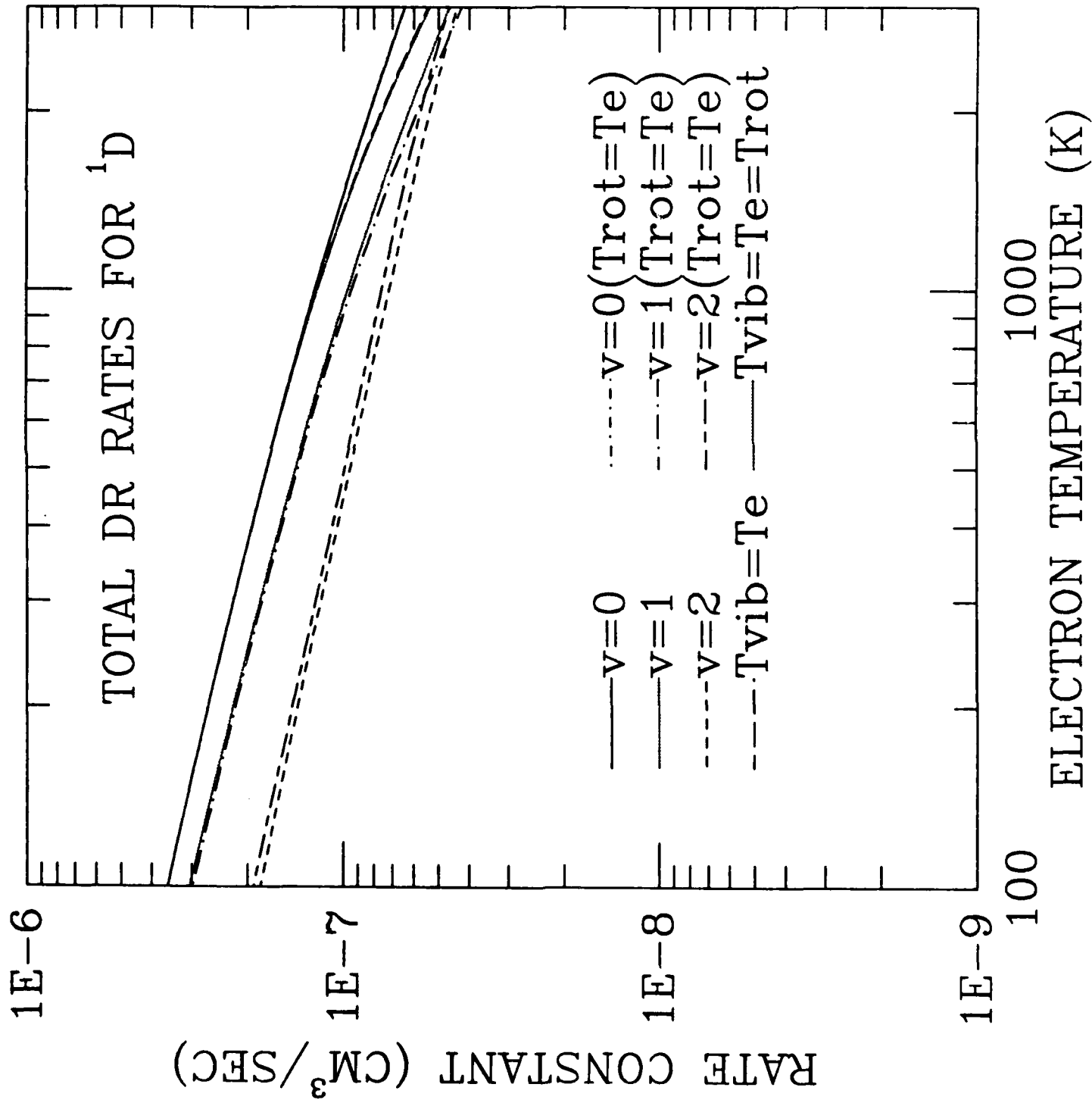
Figure Captions

1. Potential energy curves for DR leading to $O(^1D)$. The three important
calculated repulsive routes for DR of the lowest three vibrational levels are
shown. The bound potential for the ion is taken from Krupenie (1972) and
calculated points (Guberman, to be published). The vibrational wave functions
are each plotted on the same scale and are obtained from the numerical
solution of the nuclear Schroedinger equation.

2. Calculated DR rates along the $^3\Sigma_u^-$ dissociative route leading to $O(^3P)$ +
$O(^1D)$ from the lowest three vibrational levels of the ion. Also shown is the
rate for the case in which the vibrational temperature is the same as the
electron temperature. The rates are for non-rotating molecules.

3. Calculated DR rates along the $^1\Delta_u$ dissociative route leading to $O(^1D)$ +
$O(^1D)$ from the lowest three vibrational levels of the ion. Also shown is the
rate for the case in which the vibrational temperature is the same as the
electron temperature. The rates are for non-rotating molecules.

4. Calculated DR rates along the $^1\Sigma_u^+$ dissociative route leading to $O(^1S)$ +
$O(^1D)$ from the lowest three vibrational levels of the ion. Also shown is the
rate for the case in which the vibrational temperature is the same as the
electron temperature. The rates are for non-rotating molecules.

5. Calculated total DR rates for production of $O(^1D)$ from the lowest three
vibrational levels of the ion. Both the J=0 rates and rates for which the
rotational temperature is the same as the electron temperature are shown.

16

DR RATES FROM $^3\Sigma_u^-$

ELECTRON TEMPERATURE (K)

RATE CONSTANT (CM^3/SEC)

v=0
v=1
v=2
Tvib=Te

DR RATES FROM $^1\Delta_u$

v=0 ——
v=1 ——
v=2 -----
Tvib=Te ----

ELECTRON TEMPERATURE (K)

RATE CONSTANT (CM^3/SEC)

DR RATES FROM $^1\Sigma_u^+$

v=0
v=1 ----- v=2
------- Tvib=Te

RATE CONSTANT (CM³/SEC)

ELECTRON TEMPERATURE (K)

TOTAL DR RATES FOR ^{1}D

v=0
v=1
v=2
Tvib=Te
Tvib=Te=Trot

......v=0 (Trot=Te)
-.-.-v=1 (Trot=Te)
-----v=2 (Trot=Te)
-----Tvib=Te=Trot

RATE CONSTANT (CM^3/SEC)

1E-6
1E-7
1E-8
1E-9

100
1000

ELECTRON TEMPERATURE (K)

END
DATE
FILMED
5-88
DTIC